

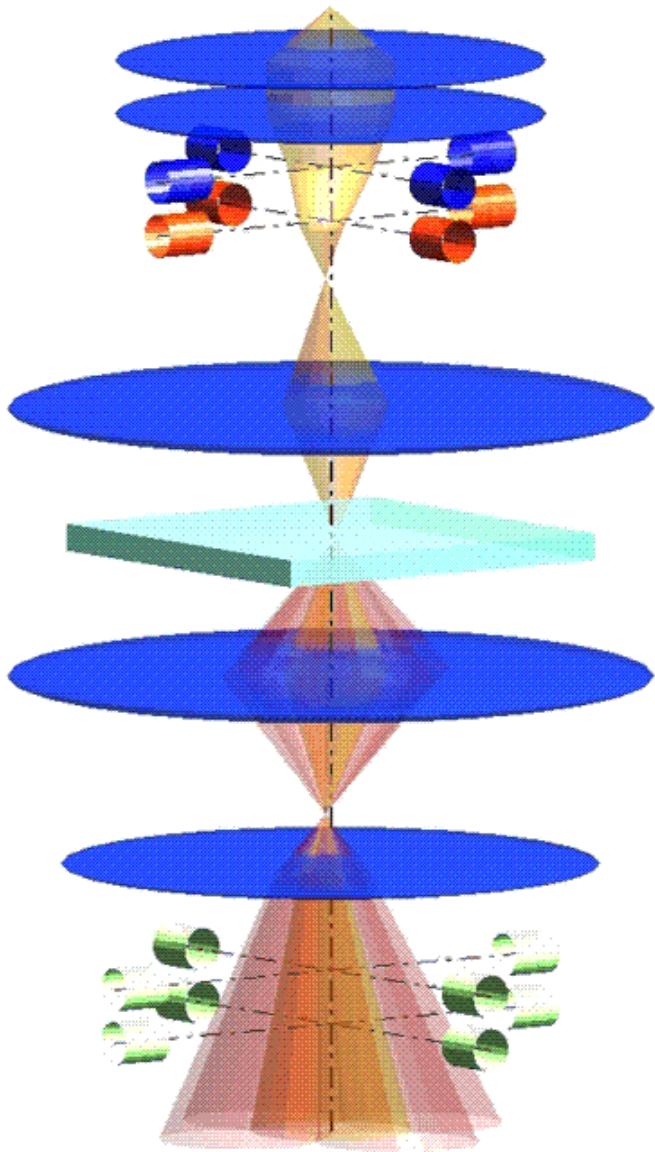
SpotMode = 0.0, DiffMode = 0.0

DiffMode = 1.0, $C_s(\text{OPF}) = 0.0 \text{ mm}$, $C_s(\text{Obj}) = 0.0$

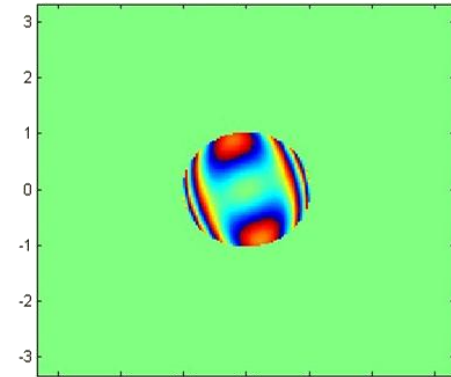
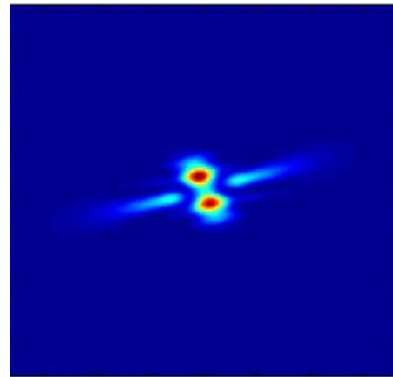
Introduction to the Theory of Image Simulation in TEM

Part I of a Pre-Congress Workshop at EMC2012 in Manchester, UK on Sept. 16, 2012

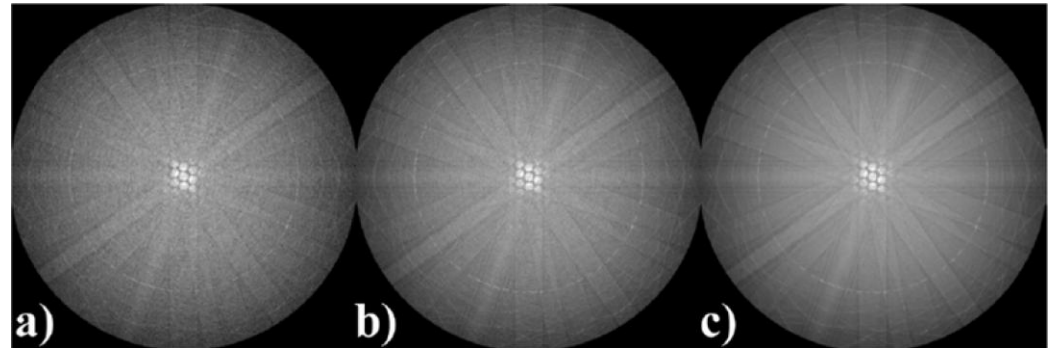
STEM Image Simulations



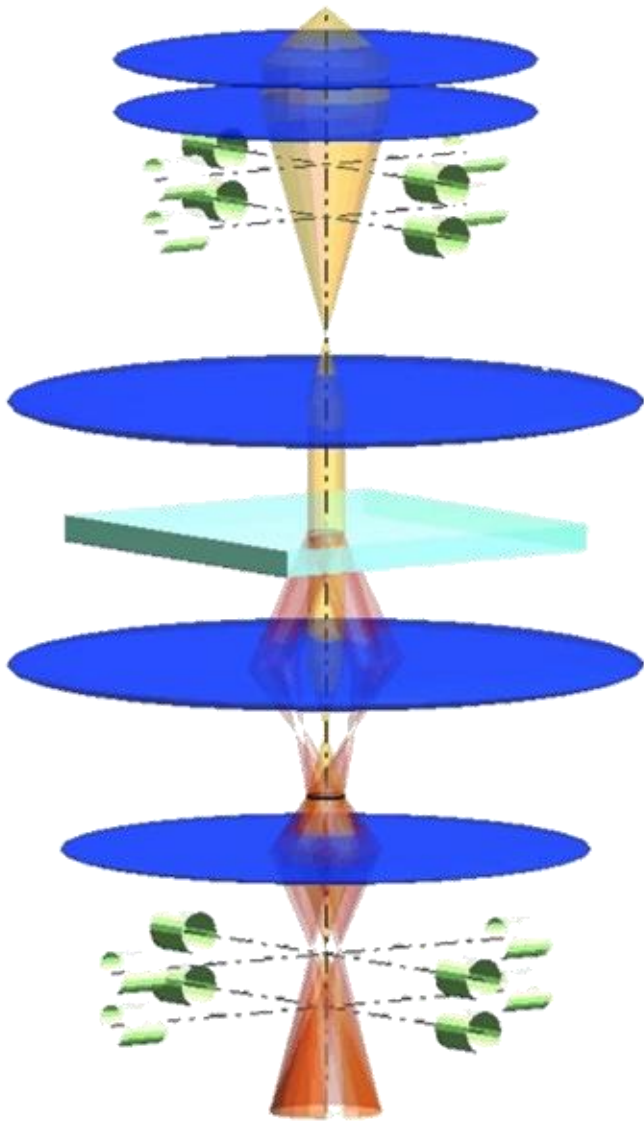
1. Probe Formation (all aberrations up to C_5)



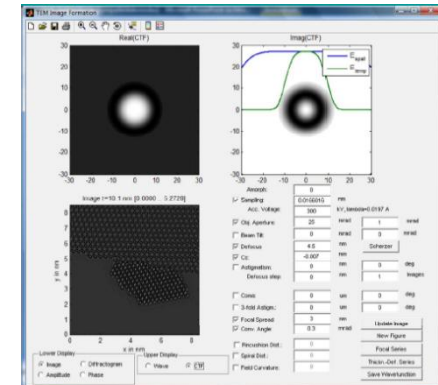
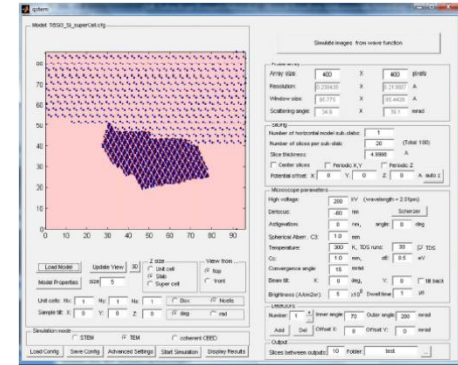
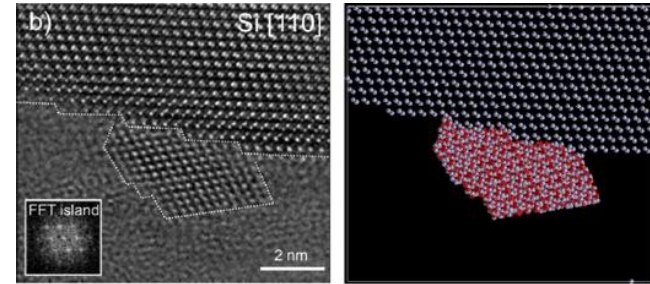
2. Thermal Diffuse Scattering (TDS)



TEM Image Simulation



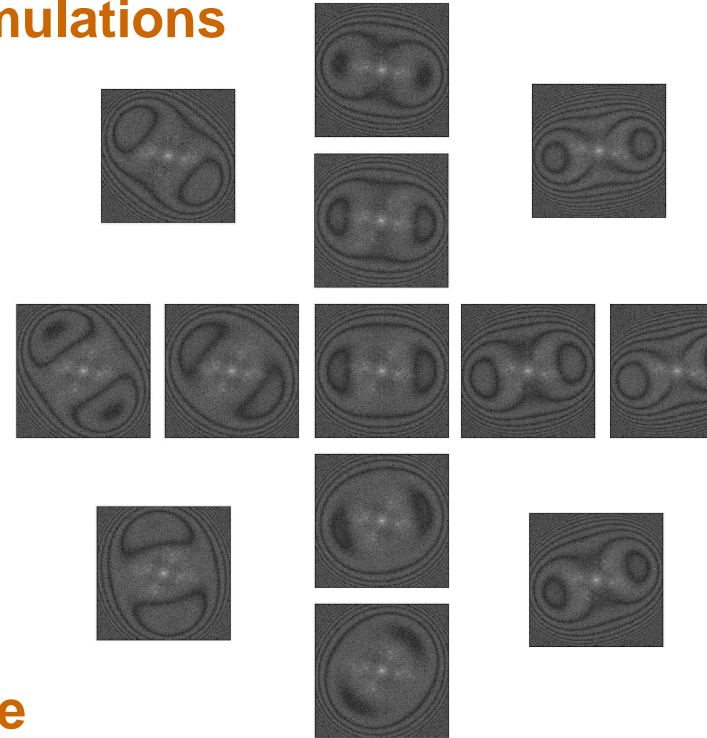
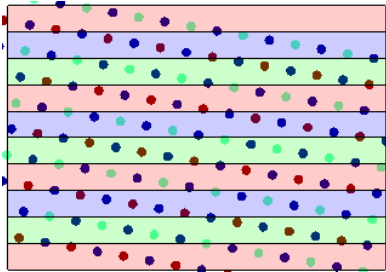
1. Build a model (possibly based on experimental observation)
2. Compute the electron scattering in the sample
3. Compute images from the exit face wave function



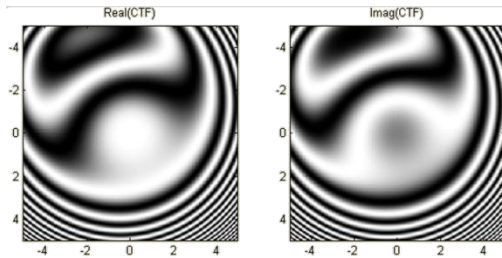
free download of the complete package at <http://elim.physik.uni-ulm.de>

Outline

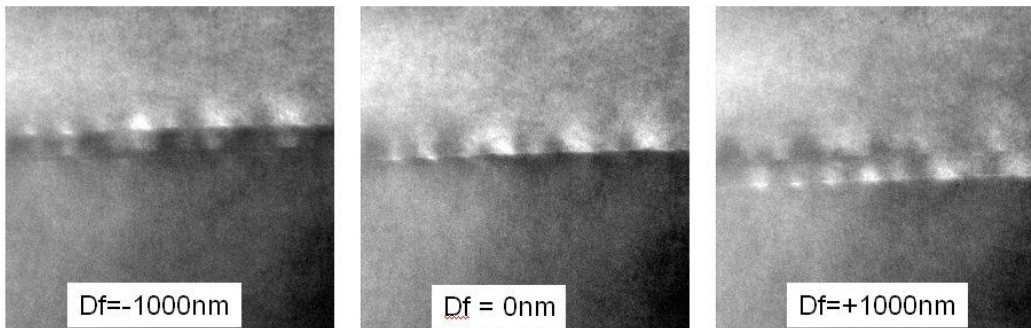
1. What to watch out for in multislice simulations



2. The wave transfer function



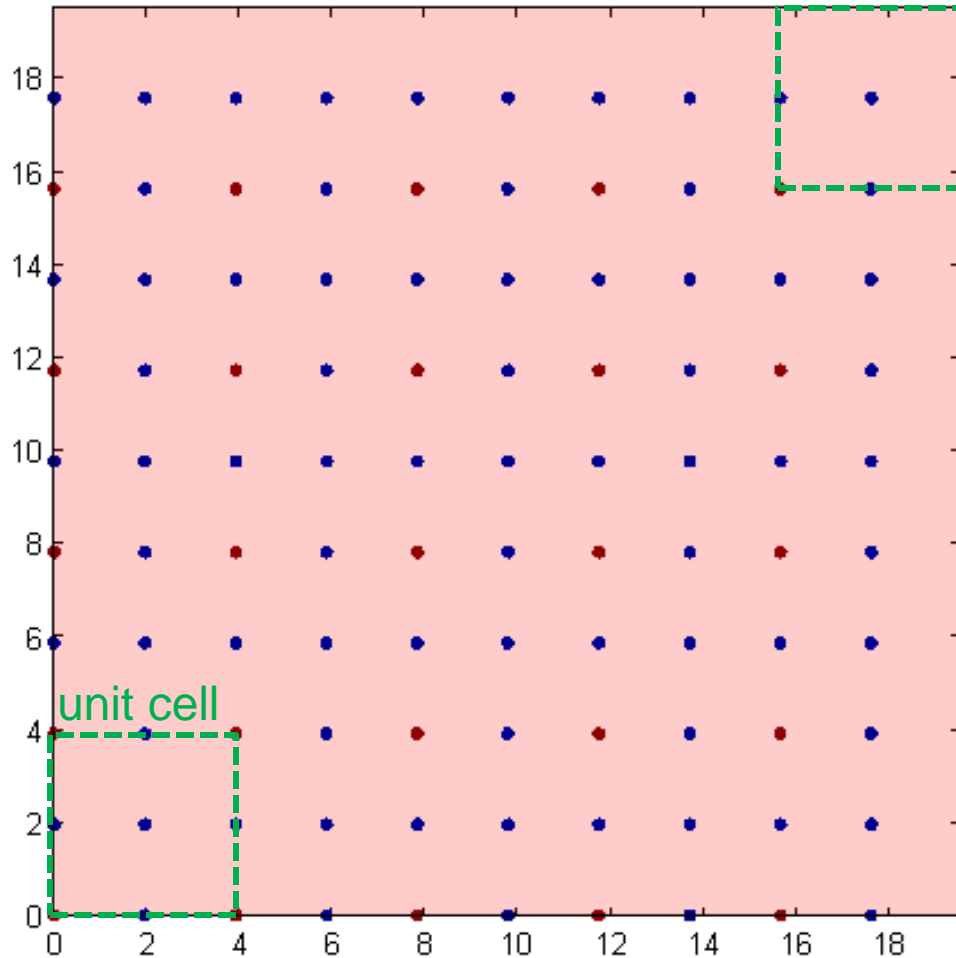
3. Partial spatial and temporal coherence



1. What to watch out for in multislice simulations

- a) How to sample the potential laterally
- b) How to slice the crystal potential longitudinally
- c) Slicing in case of defects or disordered structures
- d) Scattering factors for HAADF-STEM and phase contrast TEM
- e) Avoiding aliasing often at cost of resolution

a) How to sample the potential of super-cells laterally



- Try to make **super-cell size** integer multiple of unit cell size
- Try to make the number of **sampling points** an integer multiple of the number of unit cells

This example: 5 x 5 SrTiO₃
 => don't use 512 x 512 pixels
 but use 500 x 500 pixels

b) How to slice longitudinally (along the beam)

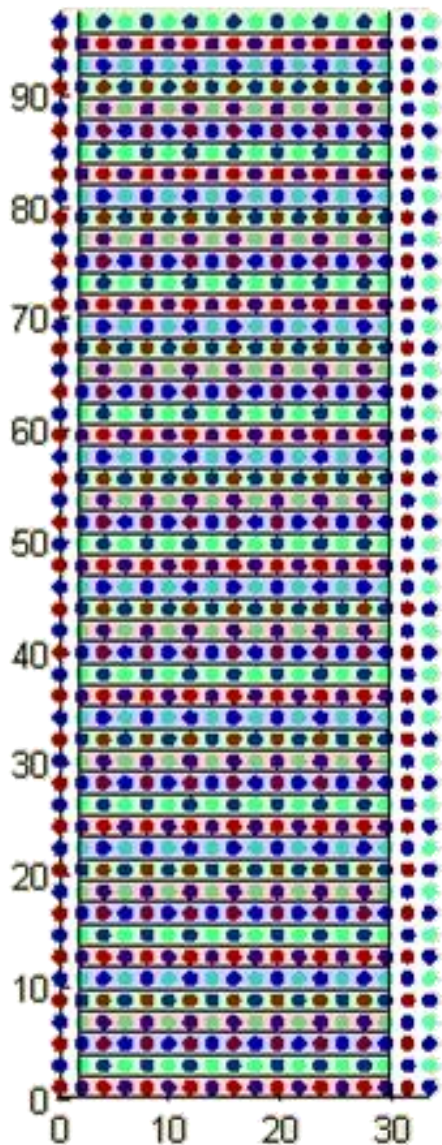
Exact zone axis

SrTiO_3

$t = 98\text{\AA}$

$\theta_y = 0^\circ$

$dz = 0.98\text{\AA}$



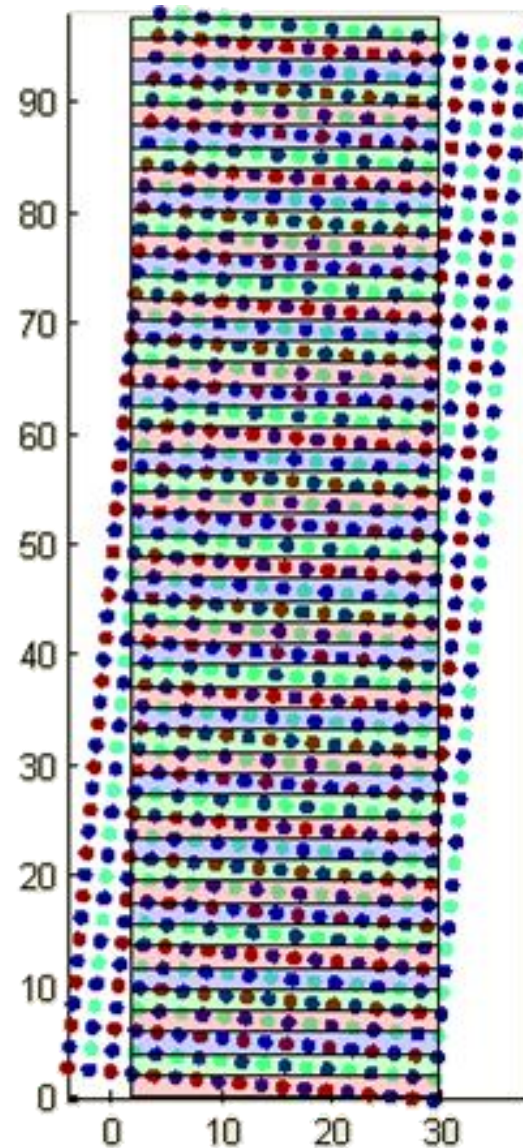
Tilted sample

SrTiO_3

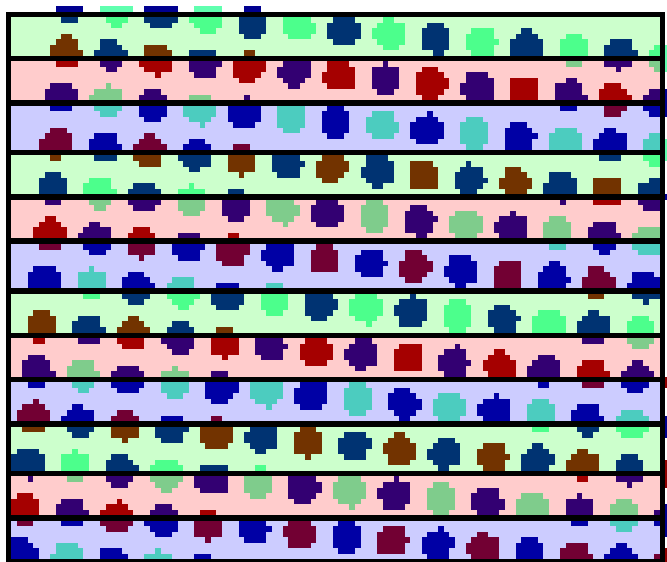
$t = 98\text{\AA}$

$\theta_y = 5^\circ$

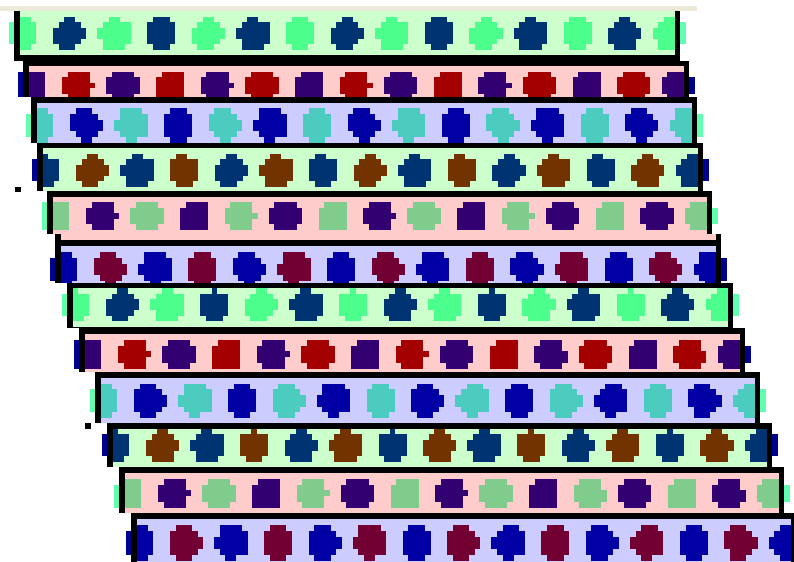
$dz = 0.98\text{\AA}$



Slice shifting



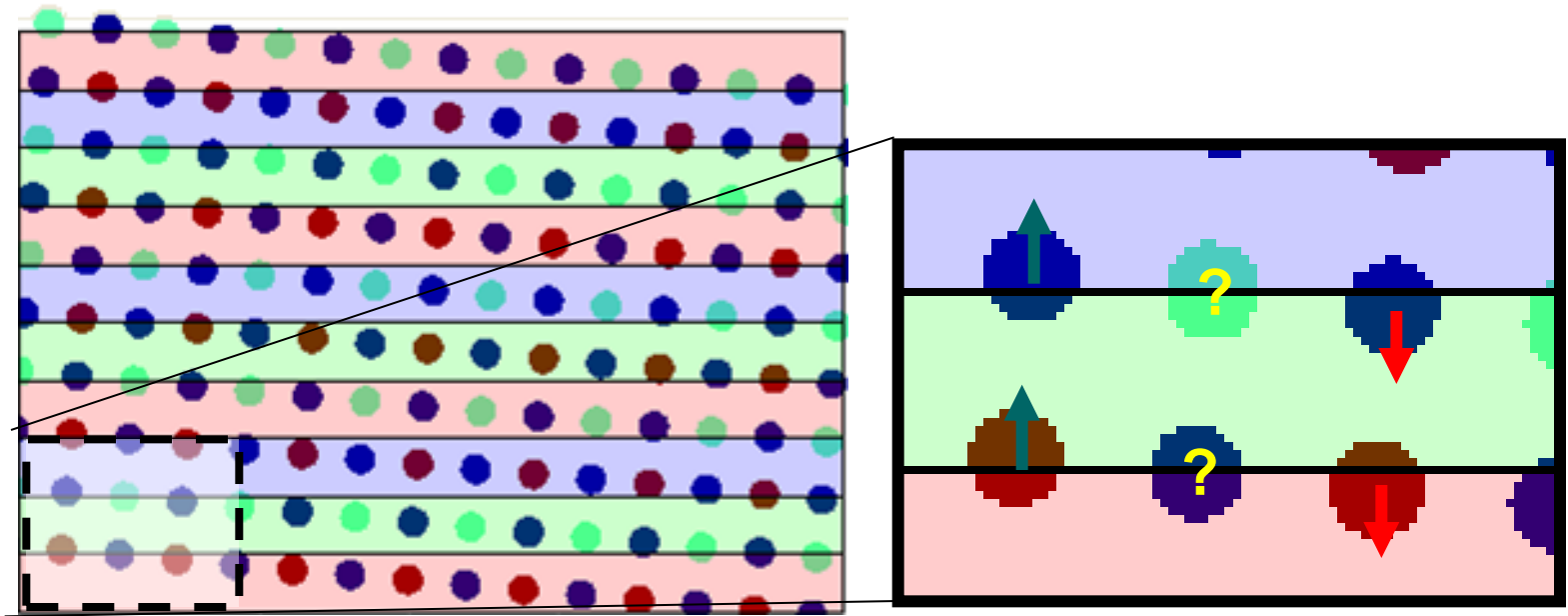
Crystal tilted 5°



Commonly used approximation:
Slice shifting
(This should only be used for
very small tilts)

QSTEM does not use slice shifting

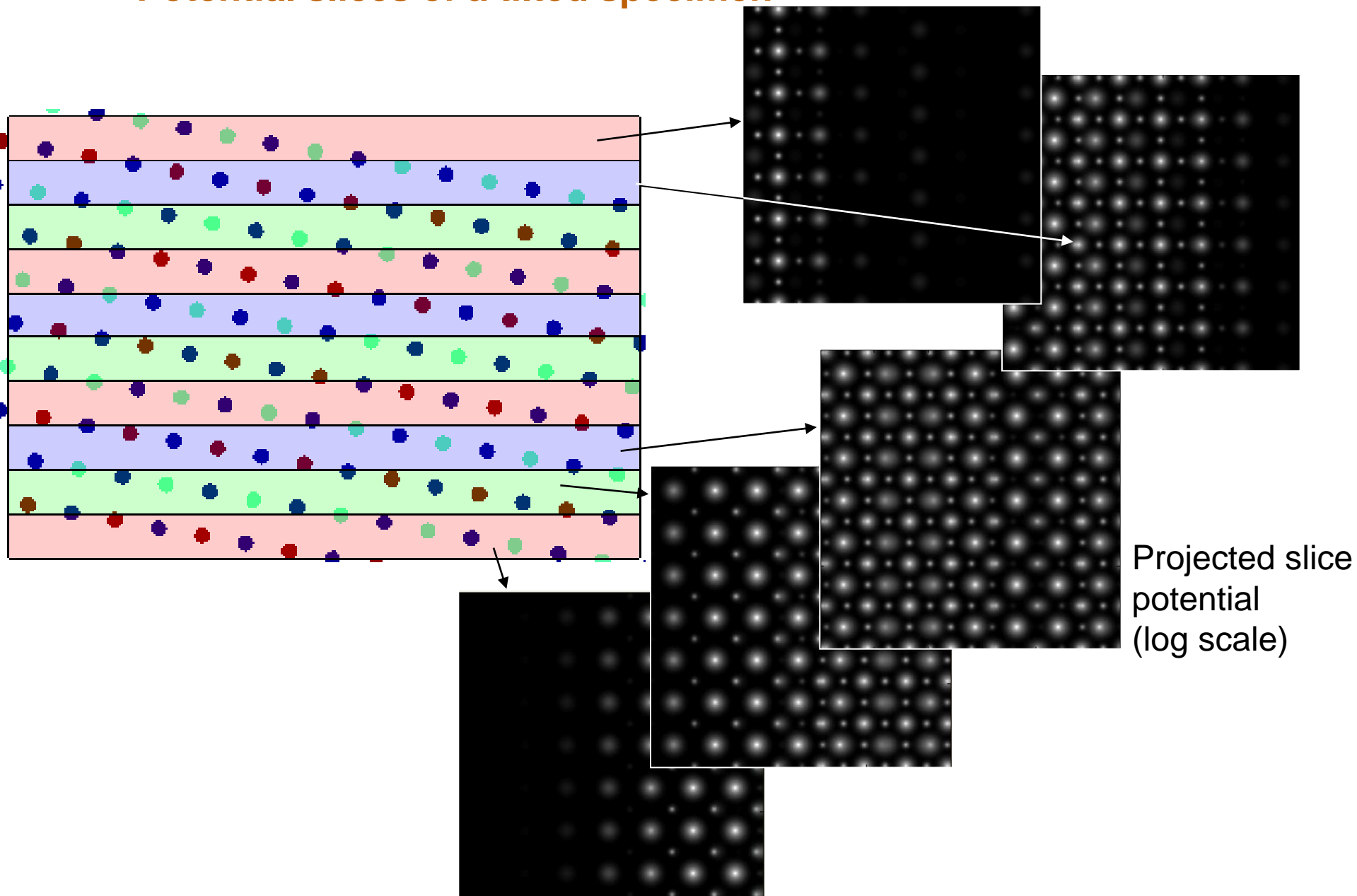
c) 3D slicing of model potential



Problem: To which slice do we assign the atomic projected potential ?

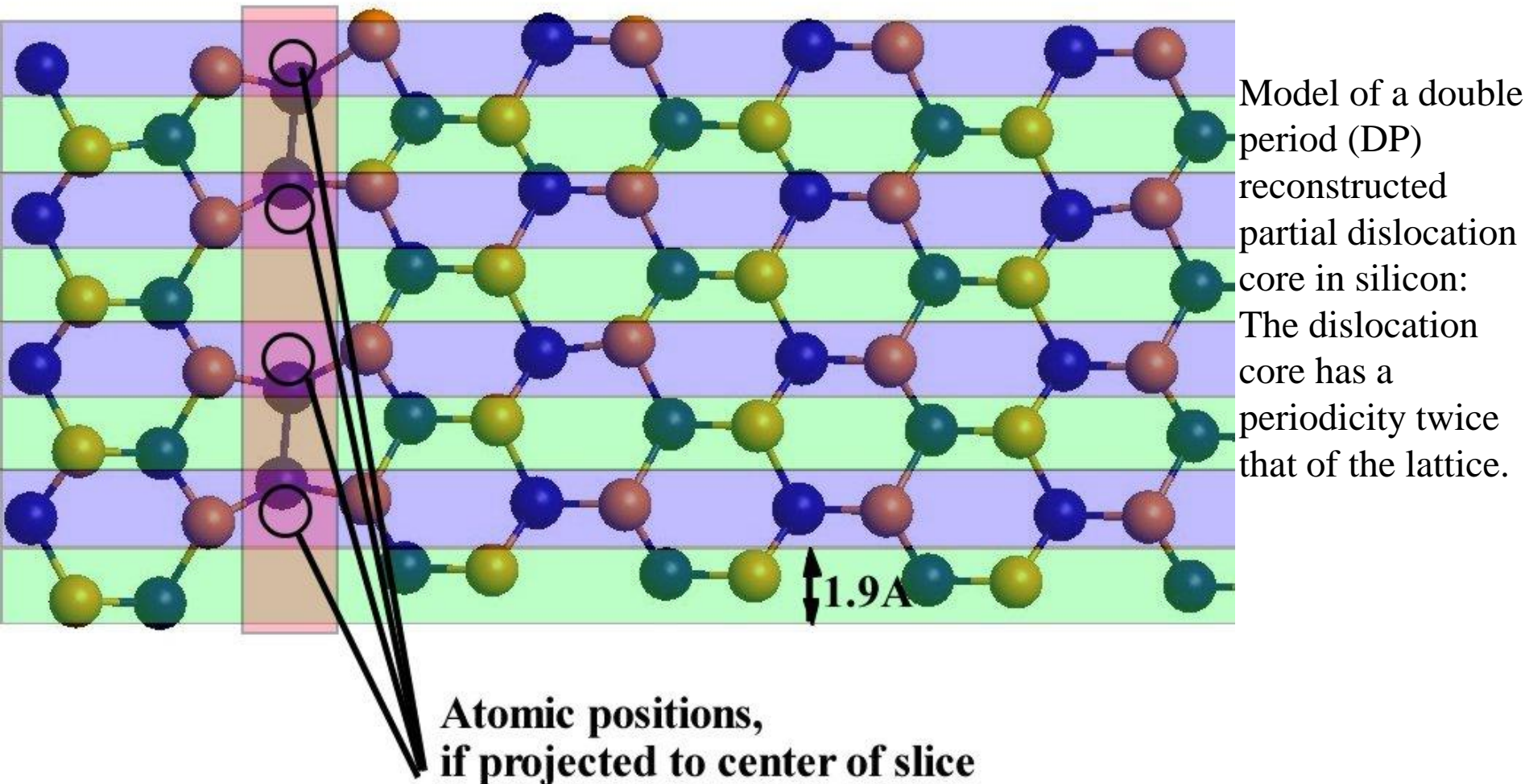
Solution: 1. Compute the 3D potential of the whole model on a fine grid.
2. Slice the 3D potential and integrate potential within each slice.

Potential slices of a tilted specimen



Exact Computation requires 3D potential

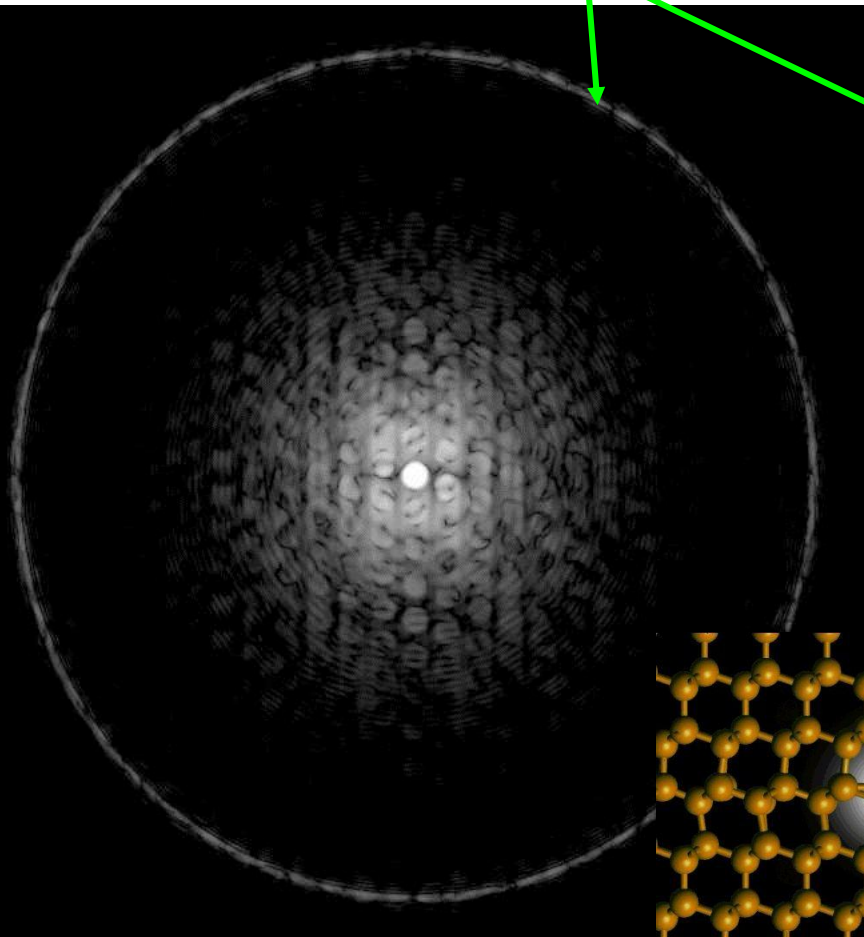
- Frozen phonon approximation for TDS simulation includes z-position.
- Electron propagation is always normal to potential slices.
- Slices can be extremely thin.



CBED patterns of 90° partial dislocation core

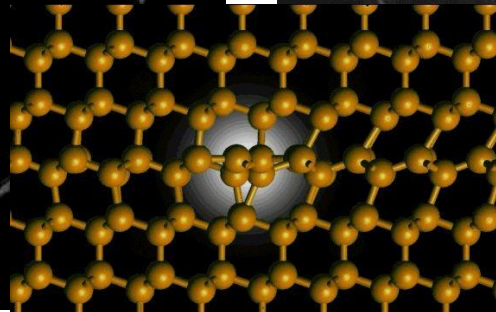
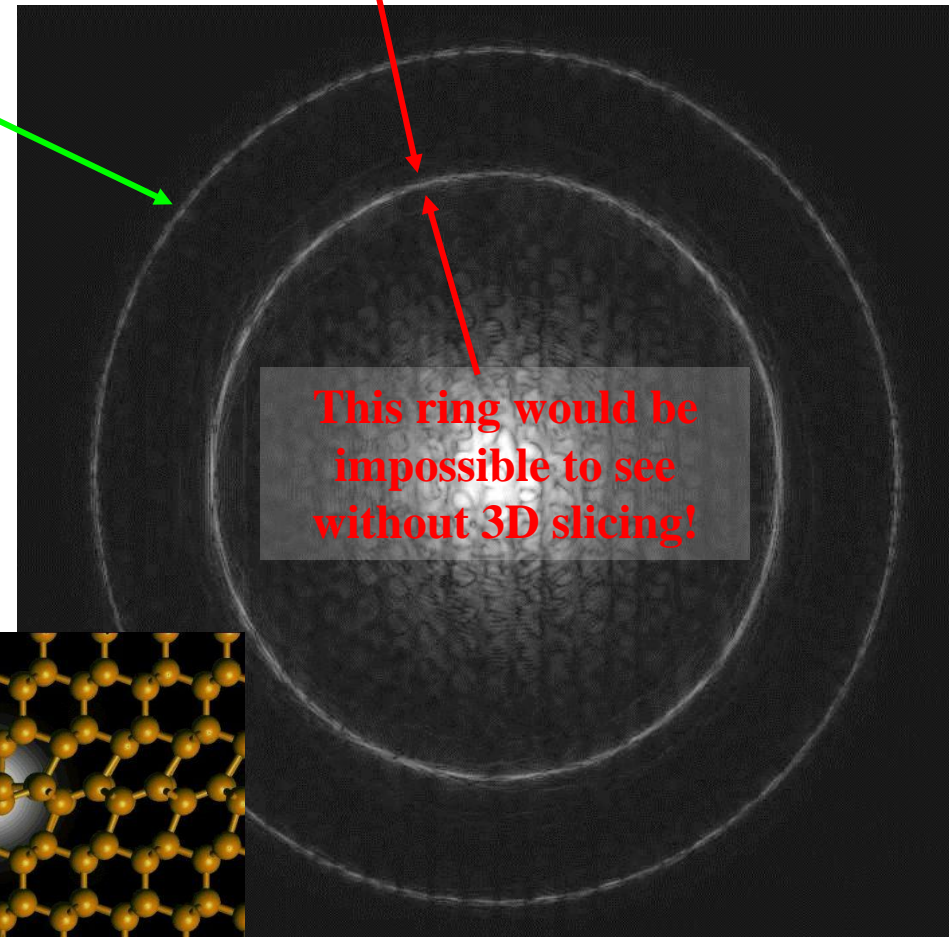
Single Period (SP) reconstruction

FOLZ ring



Double Period (DP) reconstruction

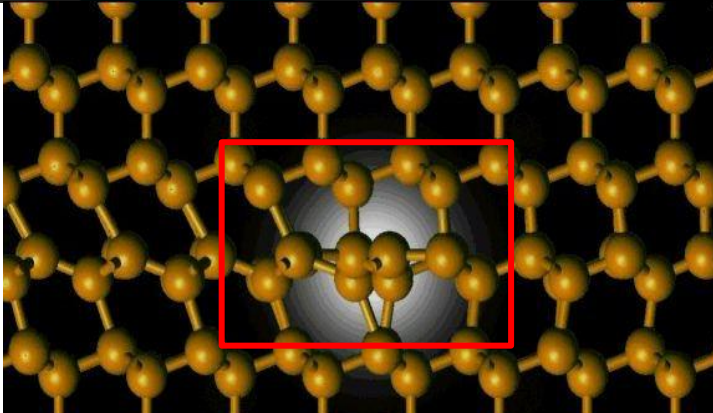
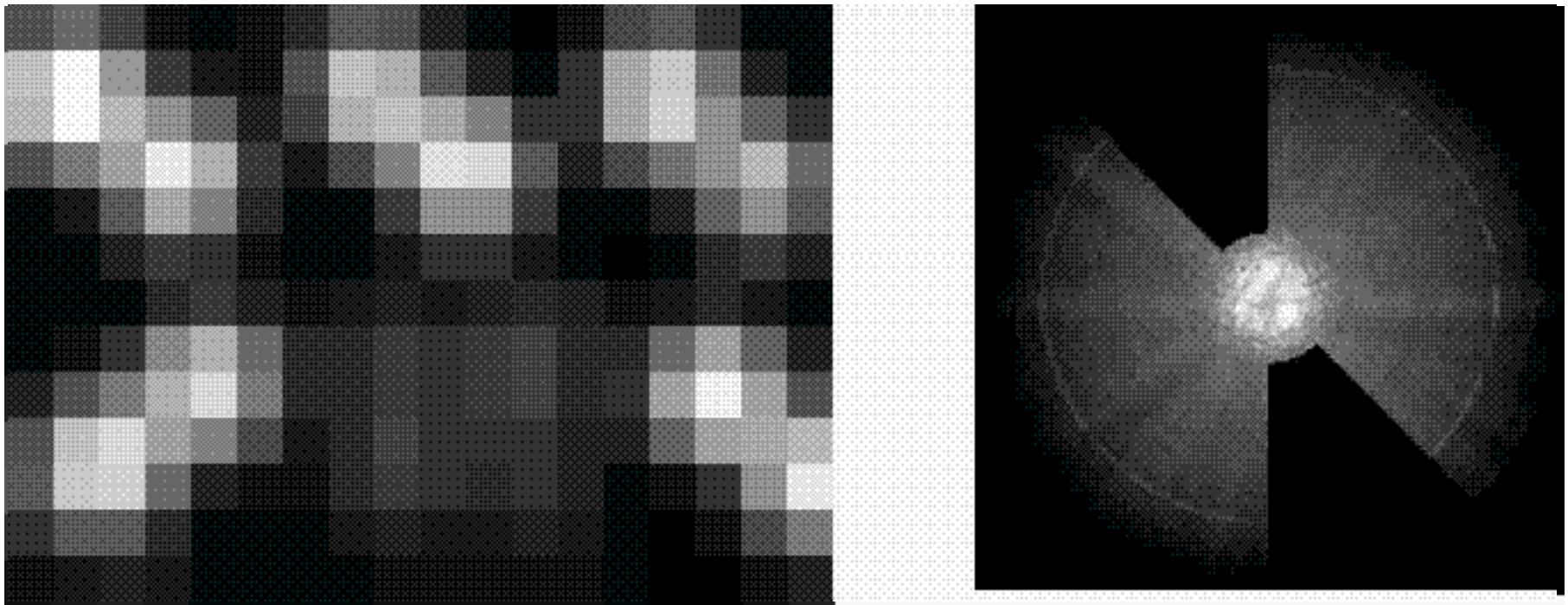
Ring of diffuse scattering



Simulation done with multislice, Debye-Waller factor: 0.44\AA^2 , **NO TDS**
thickness: 46nm (log-scale)

Z-info in HAADF-STEM images

Sample: DP-reconstructed 90° partial dislocation core in Si, viewed along (110)



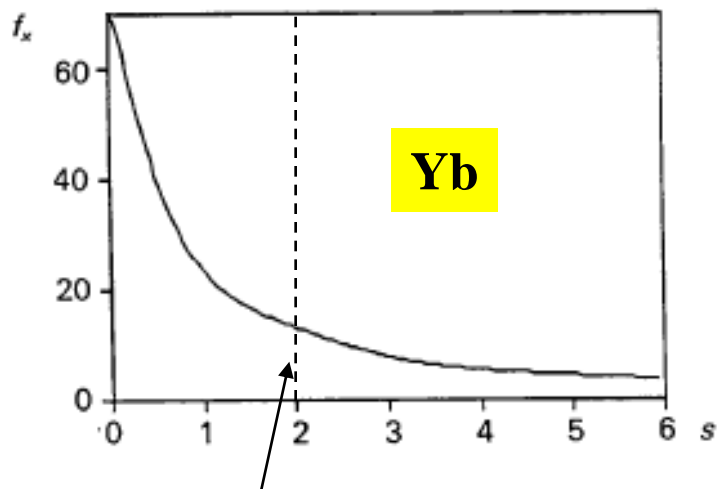
d) Scattering factors

Dirac-Fock Calculations of X-ray Scattering Factors and Contributions to the Mean Inner Potential for Electron Scattering

Rez et al, Acta Cryst A50 (1994) 481

Tabulated up to $s = \sin(\theta)/\lambda = 6.0$

(important for **HAADF-STEM** simulations)

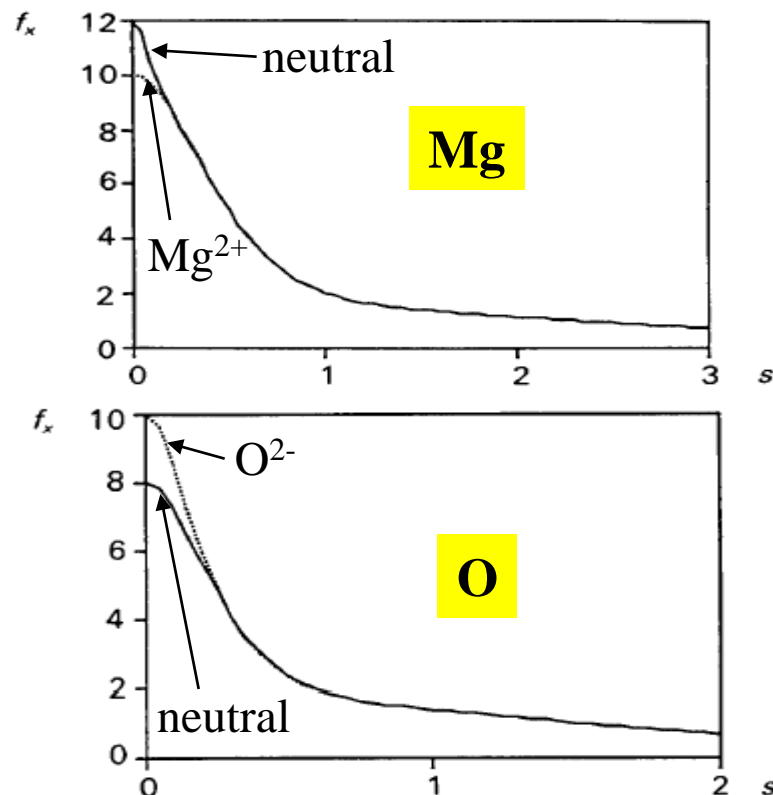


Most parameterizations
fitted up to $s=2$ only

Use Bethe-Mott formula to get $f_{el}(s)$

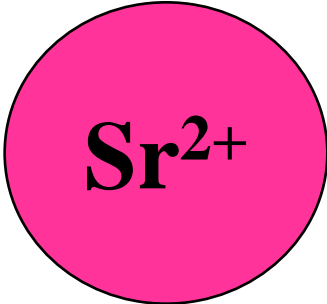

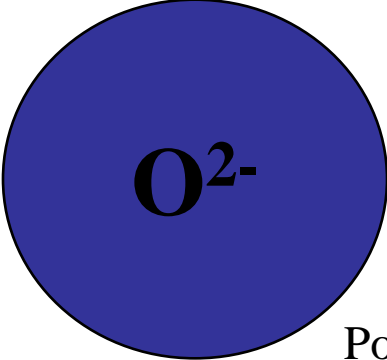
Ionic scattering factors

(important for **BF-(S)TEM** simulations)



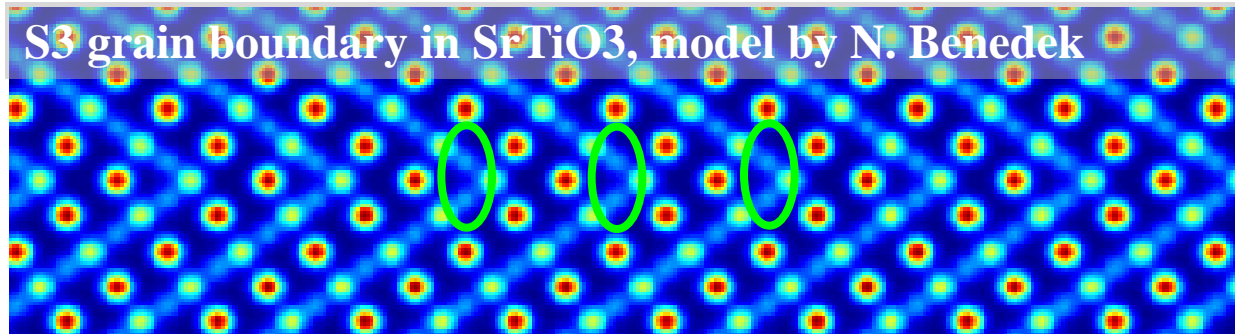
$V_0(\text{MgO}): 17.5\text{V (neutral) / 11.5V (ionic)}$

Mean Inner Potential Contribution of Ions

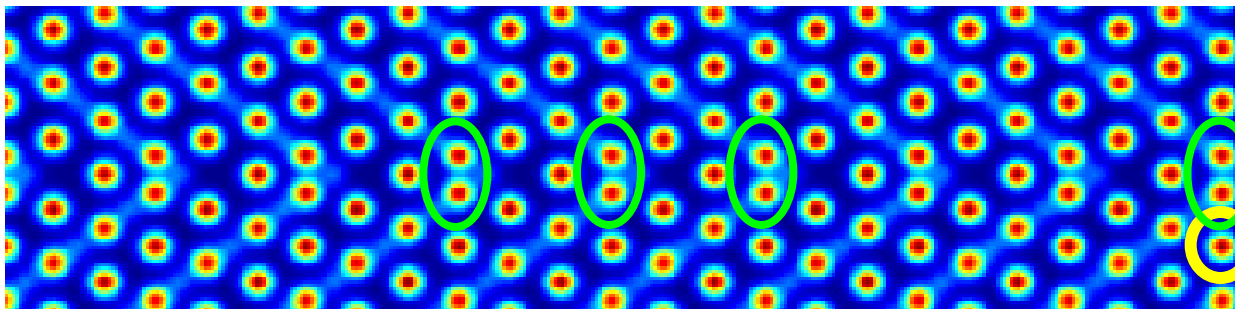
	Watson sphere radius	Total potential V_0
	118 pm	4.63 V (neutral atom: 13.0 V)
	67 pm	1.84 V (neutral atom: 8.7 V)
	140 pm	4.10 V (neutral atom: 2.0 V)

Potentials from Rez, Rez and Grant, Acta Cryst A **50** (1994) 481

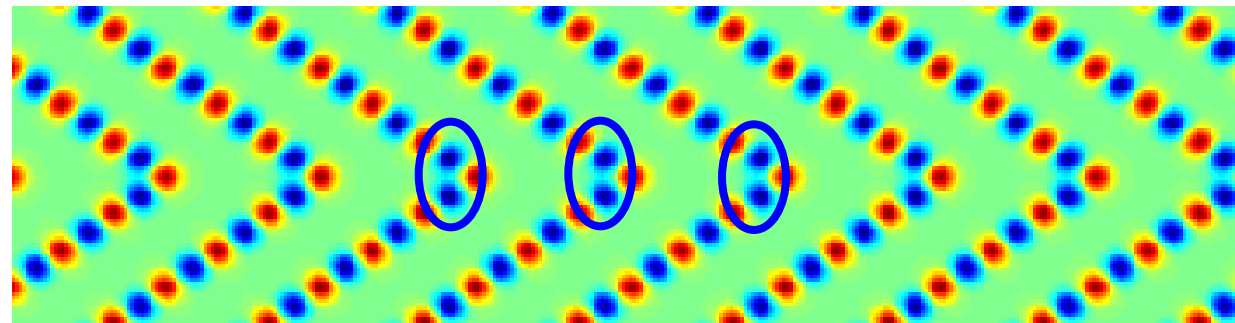
Mean inner potential: charge matters



Mean inner potential contribution
(using **neutral** atom scattering factors)



Mean inner potential contribution
(using **ionic** scattering factors)



O-containing columns have strong positive contribution to mean inner potential

Charge of atom columns

SrO columns are invisible in the charge map, because they are neutral

Phase shift of single $V_{O^{\bullet\bullet}}$ (O^{2-} vacancy)

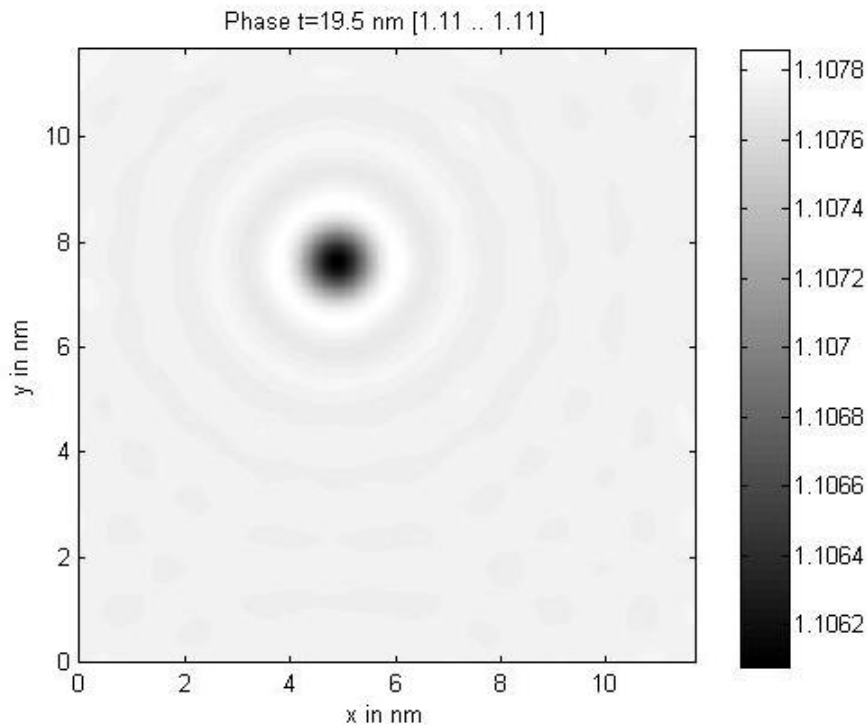
Charged ion scattering factors

Sample thickness: 20 nm

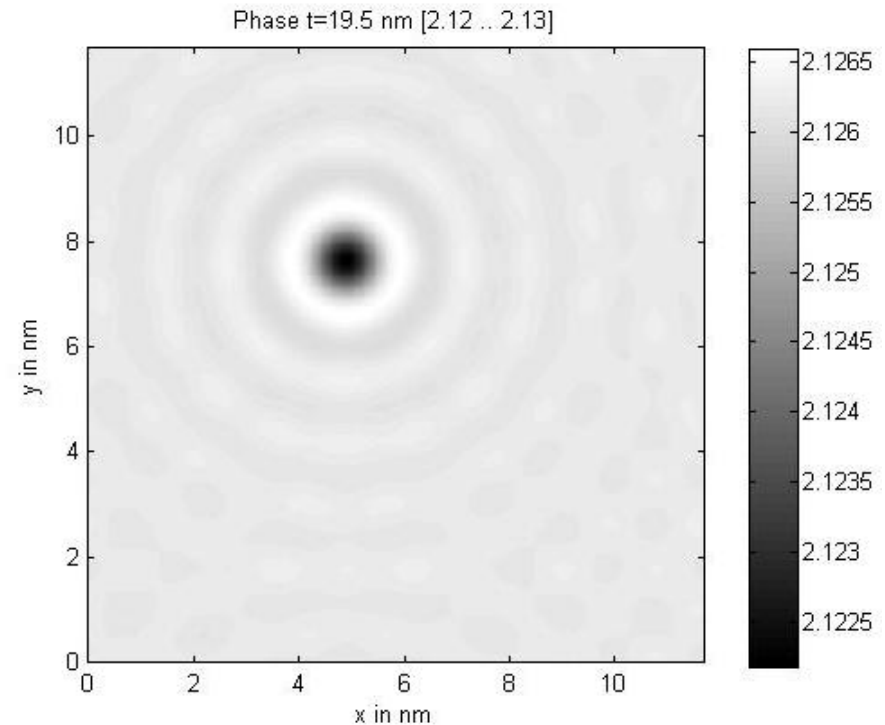
Neutral atom scattering factors

Sample thickness: 20 nm

Radius of objective aperture smaller than $\frac{1}{2}$ first Bragg angle



Phase contrast: **2 mrad**



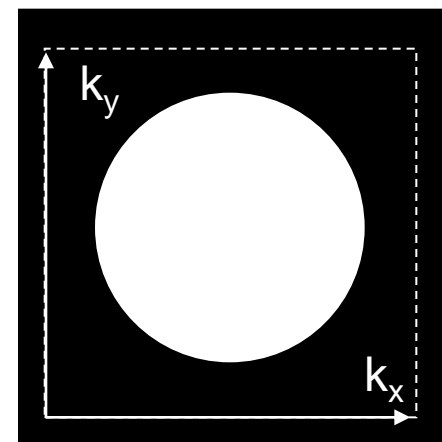
Phase contrast: **4 mrad**

Corresponding Fresnel BF-TEM contrast: 0.2 .. 0.4 %.

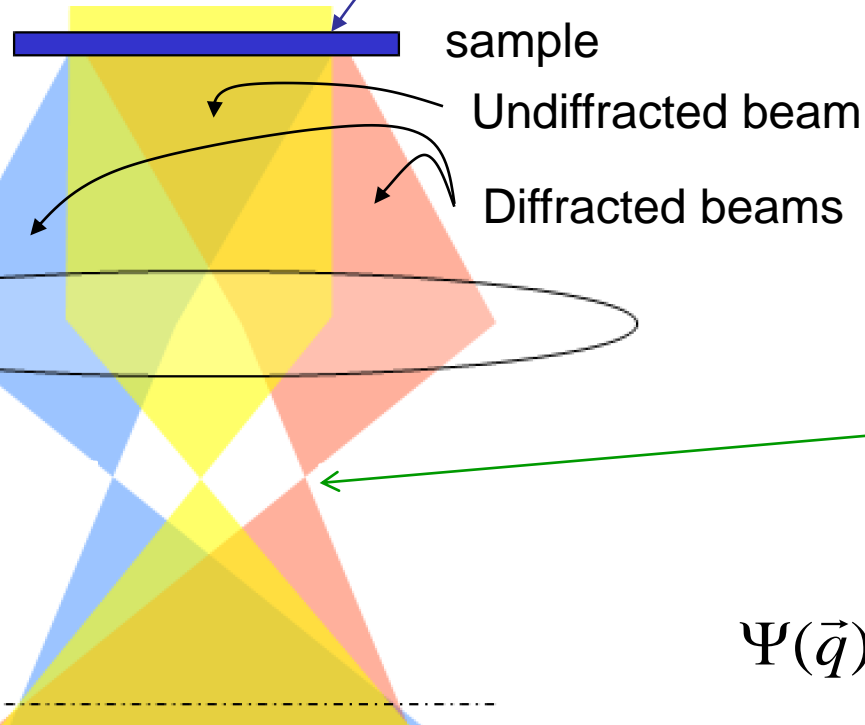
e) Avoiding aliasing often at cost of resolution

Aliasing artifacts may occur, when numerical operations on an image (or a complex wave function) are performed in reciprocal space. These effects are avoided by

1. Using bandwidth limited lookup tables for the 3-dimensional atomic potential when constructing the slices of the projected potential (no time-consuming bandwidth limiting of the final slices needs to be performed then)
2. The outer 1/3 of the wave function in k -space is set to zero after every Fresnel propagation.



2) The Wave Transfer Function & Contrast Transfer



Sample diffracts electrons, creating partial waves (beams) with different directions of propagation (\vec{q})

Diffracted beams are separated and travel different distances
=> k -dependent phase shift

$$\Psi(\vec{q}) \rightarrow \Psi(\vec{q}) \cdot e^{i\chi(\vec{q})} = \Psi(\vec{q}) \cdot e^{i\chi(\vartheta, \phi)}$$

Diffracted beams are re-united

$$\Psi'(\vec{r}) = \sum_{\vec{q}} \Psi'(\vec{q}) e^{2\pi i \vec{q} \cdot \vec{r}} = \text{FT}^{-1}[\Psi'(\vec{q})]$$

=> Lenses can be used to compute
1D & 2D Fourier Transforms

The Wave Transfer Function

Imperfect lenses are treated by perturbation of the paraxial ray equation using, for example, the following expansion (other expansions of lens aberrations exist as well):

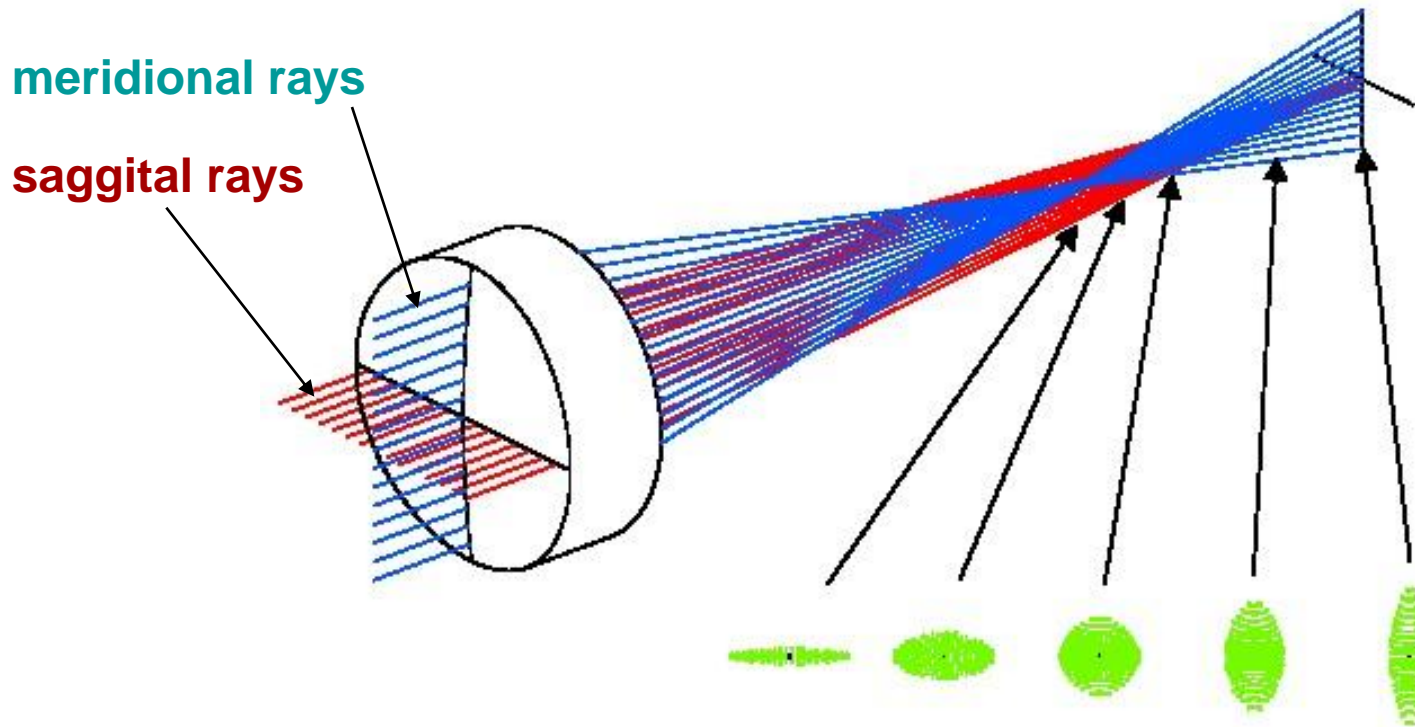
$$\begin{aligned}
 \chi(\mathcal{G}, \phi) = & |A_0| \mathcal{G} \cos(\phi - \phi_{11}) && \text{(image shift)} \\
 & + \frac{1}{2} |A_1| \mathcal{G}^2 \cos(2[\phi - \phi_{22}]) + \frac{1}{2} |C_1| \mathcal{G}^2 && \text{(astigmatism + defocus)} \\
 & + \frac{1}{3} |A_2| \mathcal{G}^3 \cos(3[\phi - \phi_{33}]) + \frac{1}{3} |B_2| \mathcal{G}^3 \cos(\phi - \phi_{31}) && \text{(3-fold astigmatism + coma)} \\
 & + \frac{1}{4} |A_3| \mathcal{G}^4 \cos(4[\phi - \phi_{44}]) + \frac{1}{4} |S_3| \mathcal{G}^4 \cos(2[\phi - \phi_{42}]) + \frac{1}{4} |C_3| \mathcal{G}^4 && \text{(..+..+ spherical aberration)} \\
 & + \frac{1}{5} |A_4| \mathcal{G}^5 \cos(5[\phi - \phi_{55}]) + \frac{1}{5} |D_4| \mathcal{G}^5 \cos(3[\phi - \phi_{53}]) + \frac{1}{5} |B_4| \mathcal{G}^5 \cos(\phi - \phi_{51}) \\
 & + \frac{1}{6} |A_5| \mathcal{G}^6 \cos(6[\phi - \phi_{66}]) + \dots && + \frac{1}{6} |C_5| \mathcal{G}^6
 \end{aligned}$$

With increasing image resolution, higher-order aberration coefficients become important.

The spherically symmetric aberrations (C_3 , C_5 , ...) are present even in perfect (round) lenses. Special correcting elements must therefore be designed to correct for them.

$$\mathcal{G} = \sin^{-1}(|q| \lambda) \approx |q| \lambda \qquad \phi = \tan^{-1}(q_y / q_x)$$

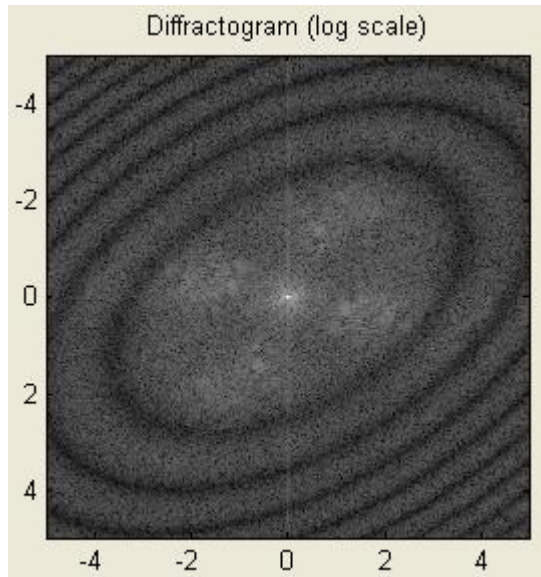
Astigmatism



Electrons passing at different directions away from the optic axis have different focal lengths.

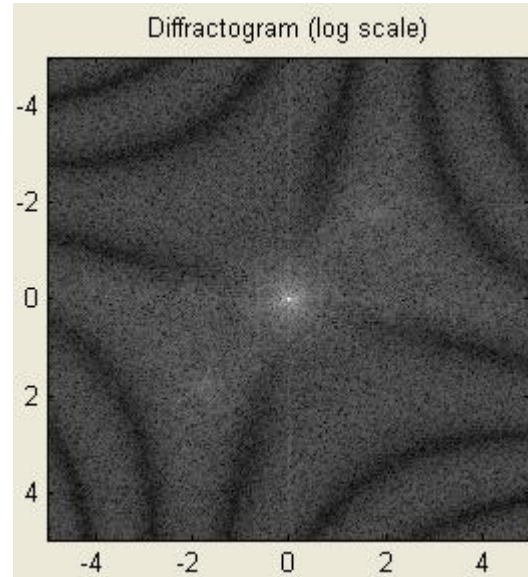
Aberration (or “phase distortion”) function:
$$\chi(\mathcal{G}, \varphi) = \frac{1}{2} |A_1| \mathcal{G}^2 \cos(2[\varphi - \varphi_{22}])$$

Effect of Astigmatism



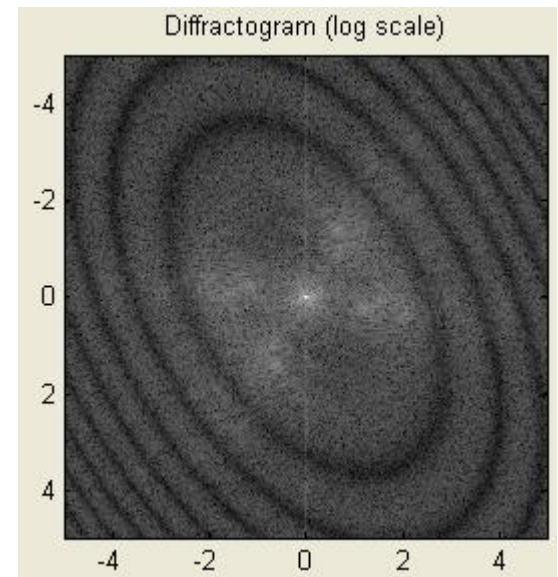
$$\Delta f = 50 \text{ nm}, |A_1| = 25 \text{ nm}$$

$$\phi_{22} = 30^\circ$$



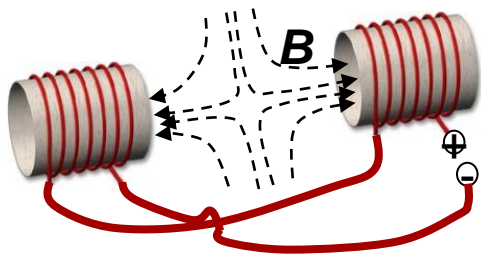
$$\Delta f = 0 \text{ nm}, |A_1| = 25 \text{ nm}$$

$$\phi_{22} = 30^\circ$$



$$\Delta f = -50 \text{ nm}, |A_1| = 25 \text{ nm}$$

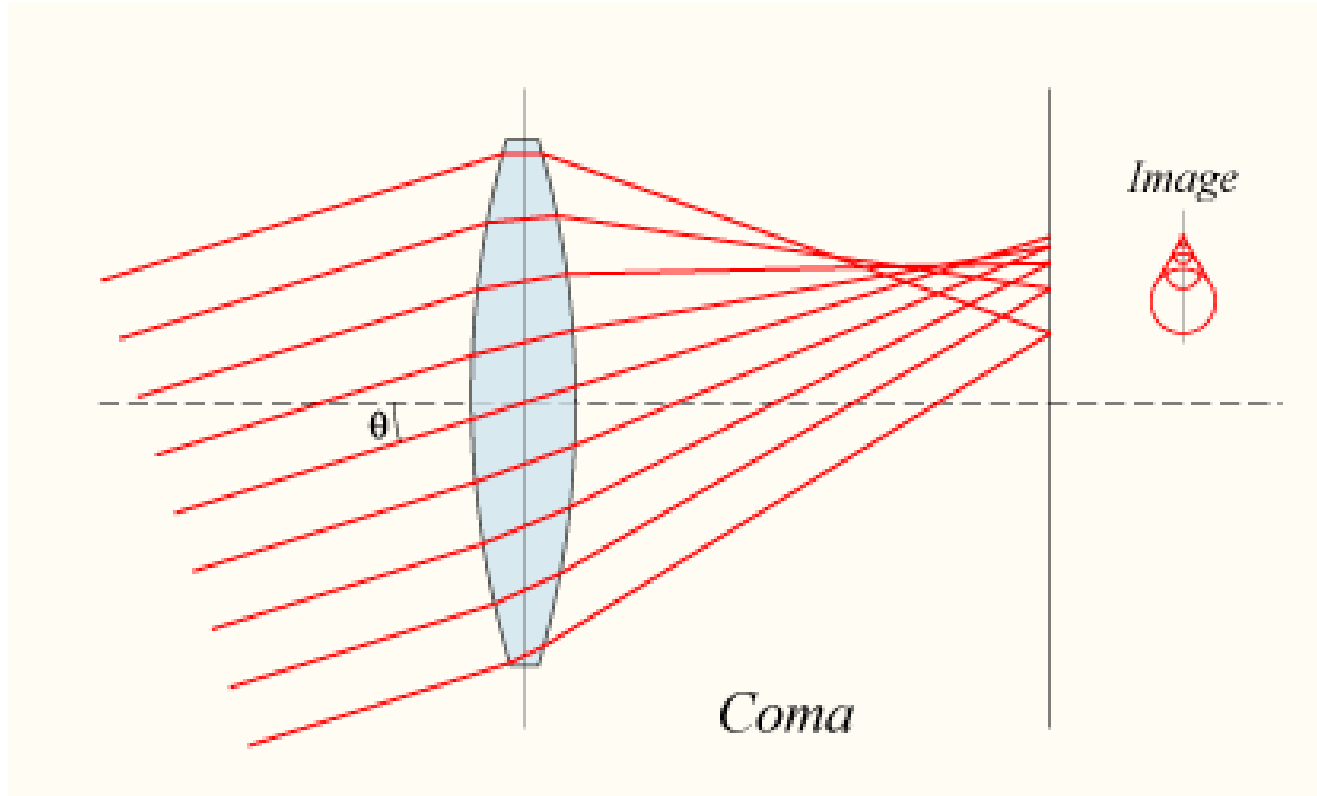
$$\phi_{22} = 30^\circ$$



Astigmatism is most easily corrected by switching between over- and under focus and making the diffractogram round for both using the stigmator (quadrupole) coils.

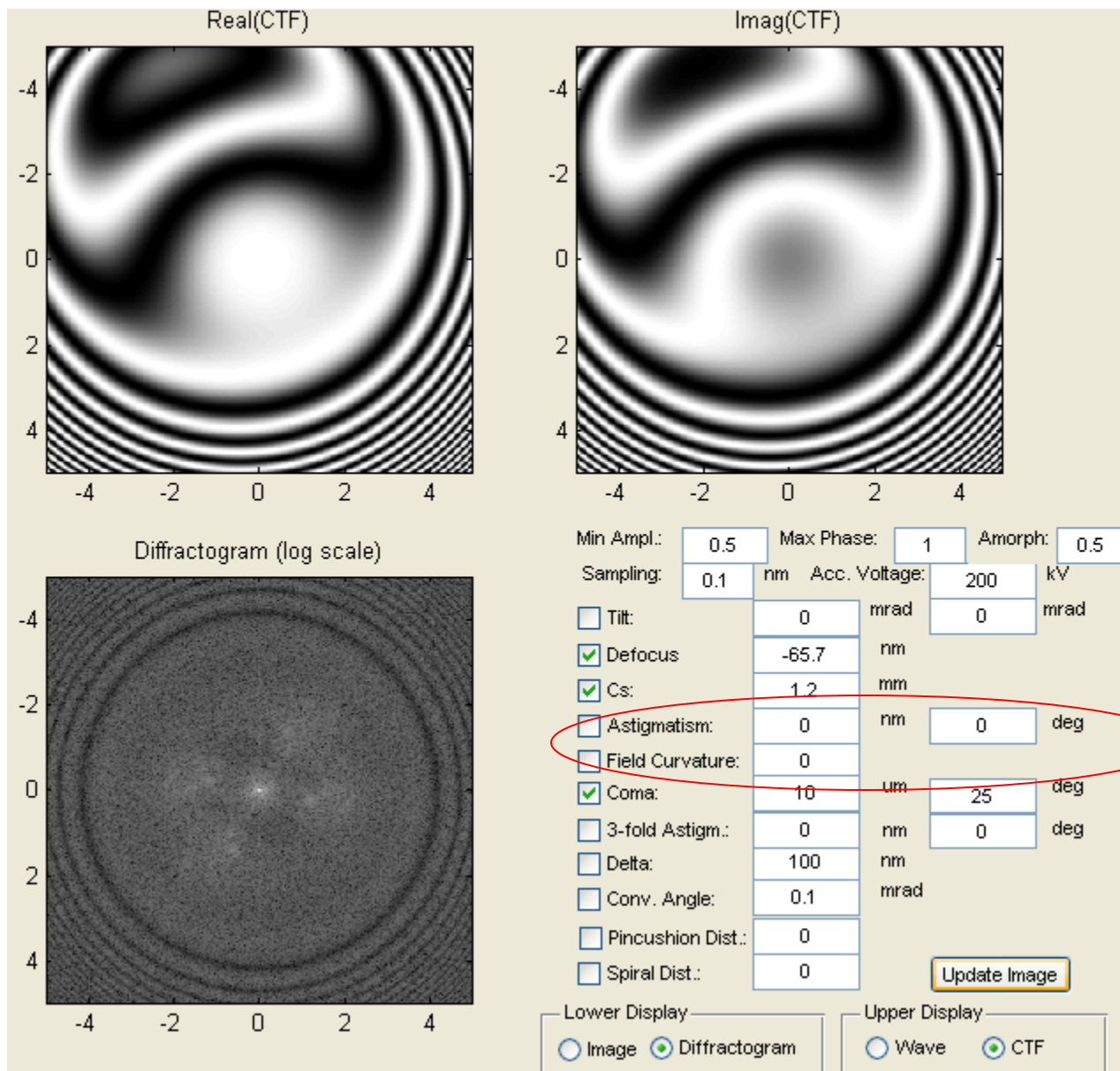
Coma

Coma is defined as a variation in magnification over the entrance pupil

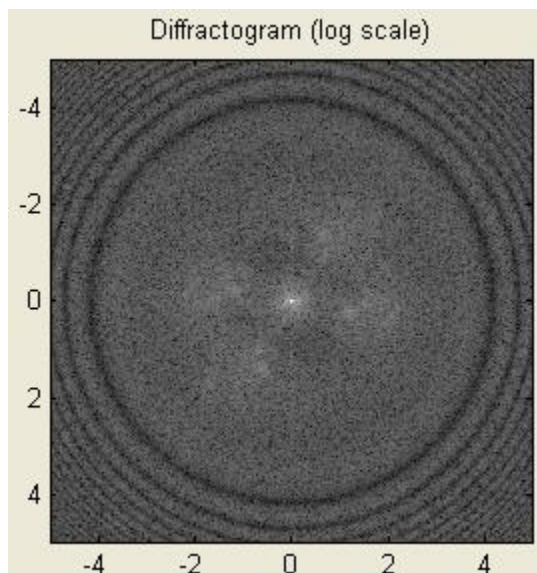


$$\chi(\mathcal{G}, \phi) = \frac{1}{3} |B_2| \mathcal{G}^3 \cos(\phi - \phi_{31})$$

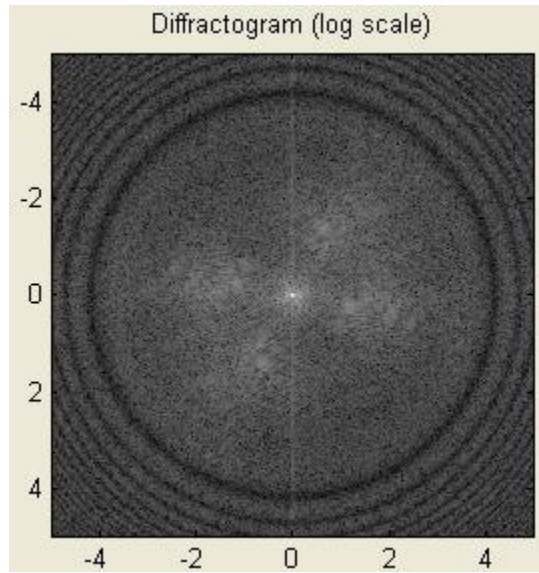
Effect of Coma



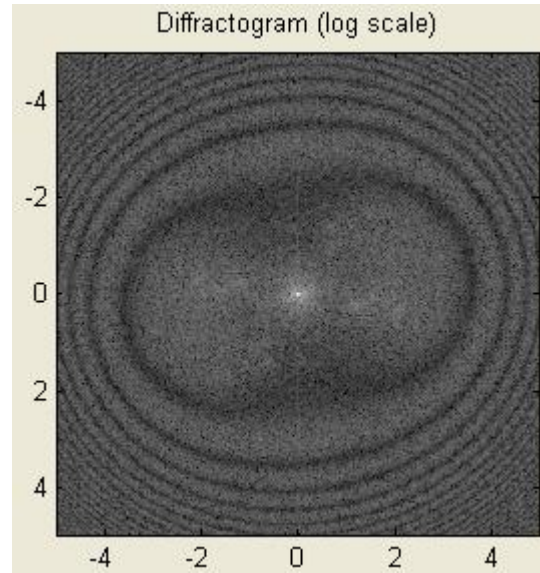
Asymmetric Aberrations only visible with Tilt



$C_s = 1.2\text{mm}$, $\Delta f = -65.7\text{nm}$,
 $B_2 = 10\mu\text{m}$, Tilt=(0,0)mrad



$C_s = 1.2\text{mm}$, $\Delta f = -65.7\text{nm}$,
 $B_2 = 0\mu\text{m}$, Tilt=(0,0)mrad



$C_s = 1.2\text{mm}$, $\Delta f = -65.7\text{nm}$,
 $B_2 = 10\mu\text{m}$, Tilt=(2,0)mrad

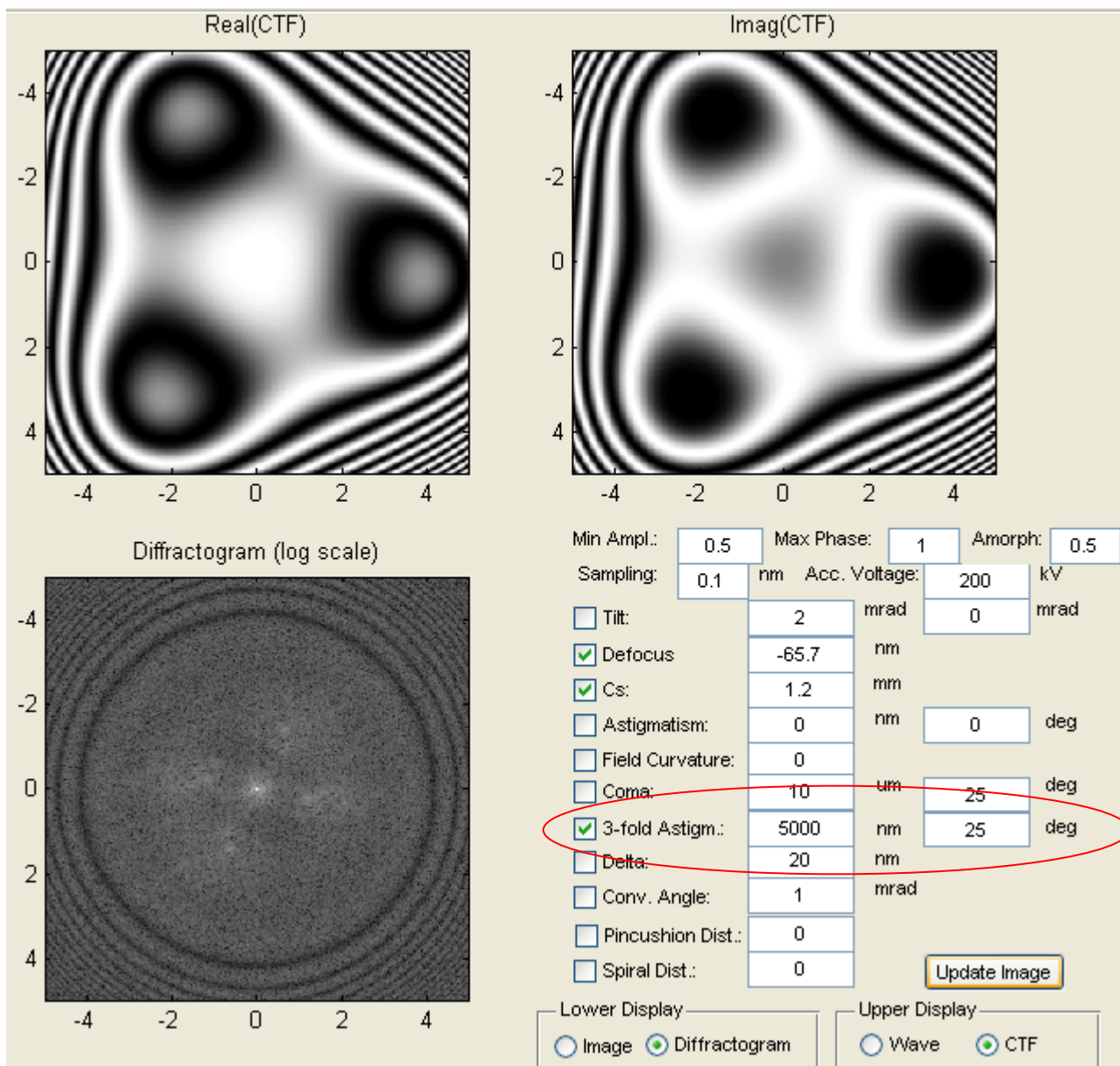
Asymmetric aberrations may reduce the contrast in the diffractogram, but do not alter its shape.

Coma and **tilt** may appear as **astigmatism** in the diffractogram

3-fold Astigmatism

$$\chi(\mathcal{G}, \phi) = \frac{1}{3} |A_2| \mathcal{G}^3 \cos(3[\phi - \phi_{33}])$$

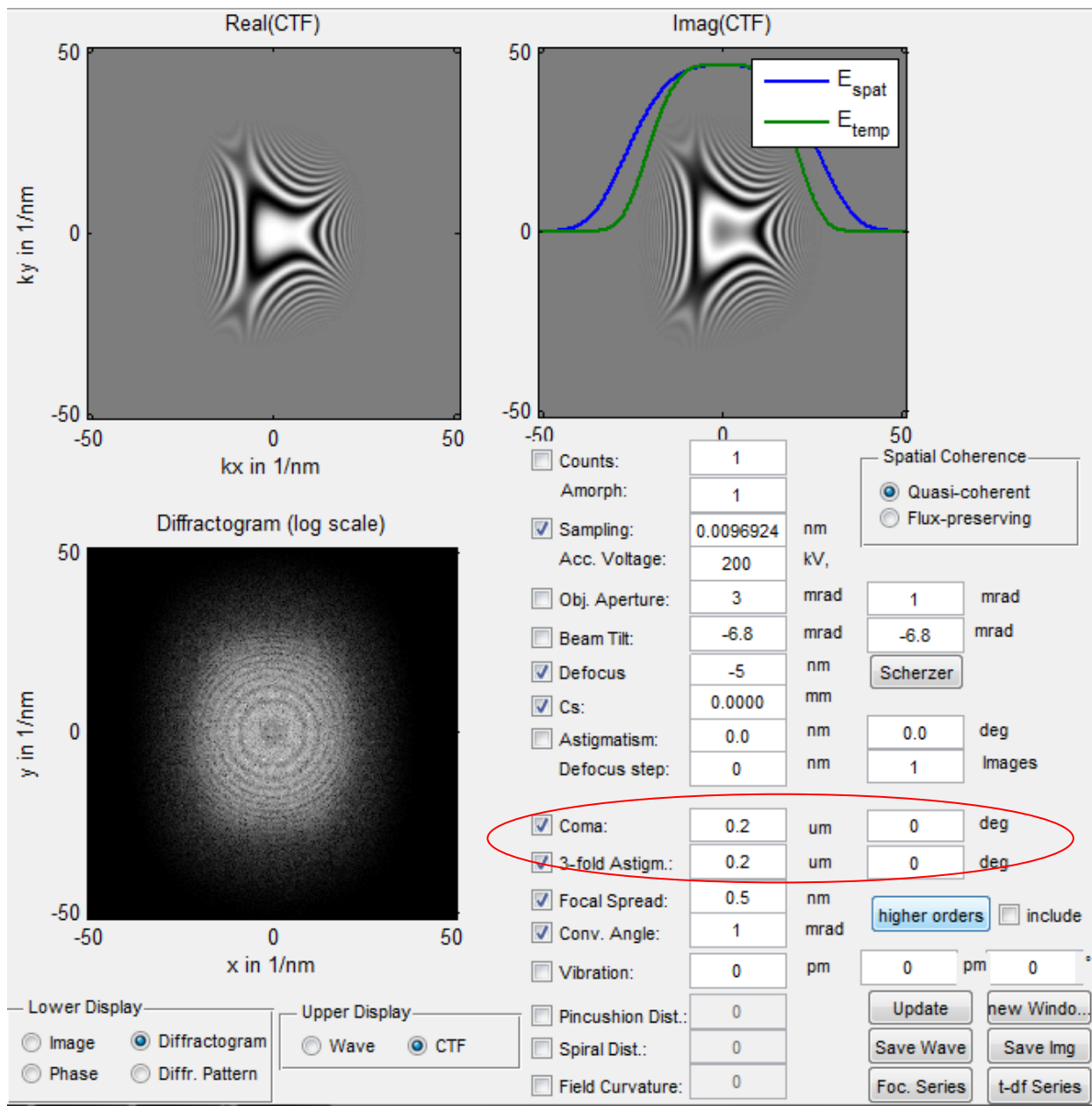
3-fold astigmatism, being an asymmetric aberration, is not visible in the geometry of the diffractogram



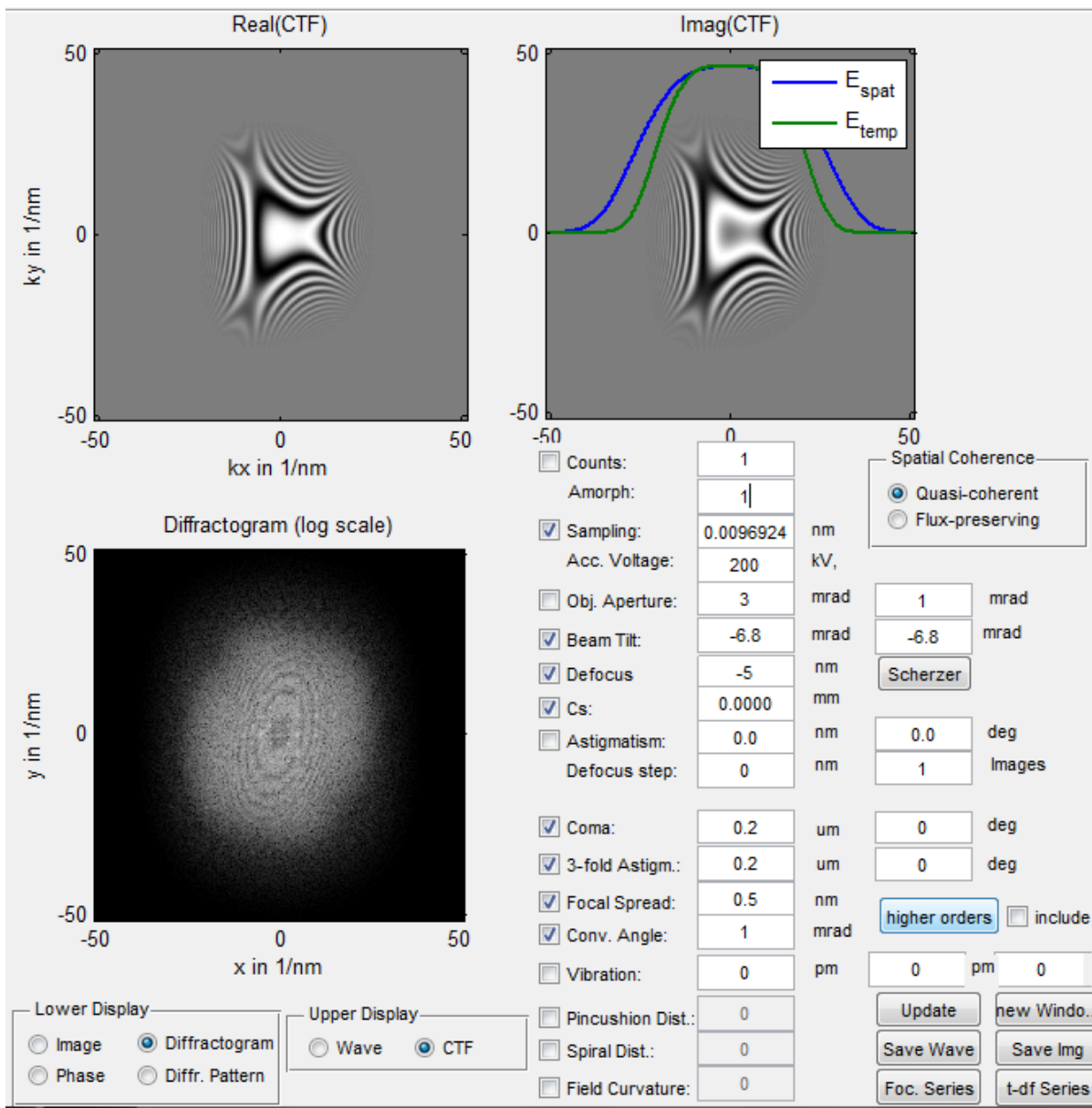
3-fold Astigmatism + Coma

$$\chi(\mathcal{G}, \phi) = \frac{1}{3} |A_2| \mathcal{G}^3 \cos(3[\phi - \phi_{33}])$$

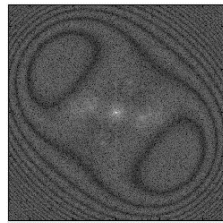
3-fold astigmatism, being an asymmetric aberration, is not visible in the geometry of the diffractogram



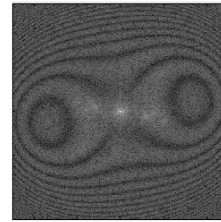
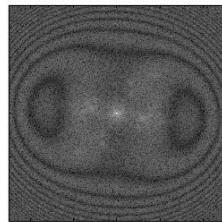
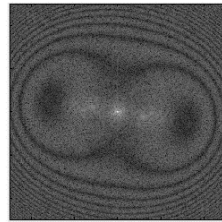
Asymmetric Aberrations Visible in Diffractogram when Tilted



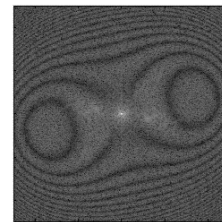
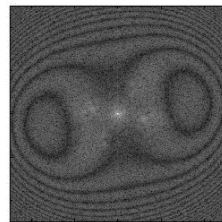
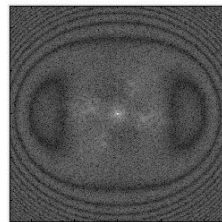
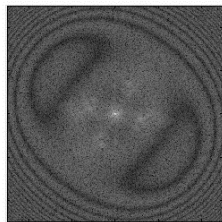
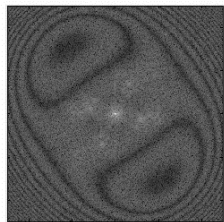
Zemlin Tableau



Tilt = $(-1.5, -1.5)$ mrad

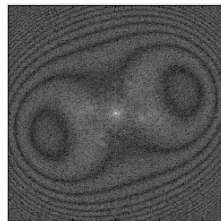
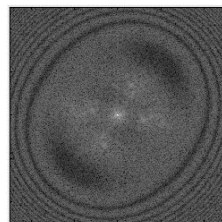
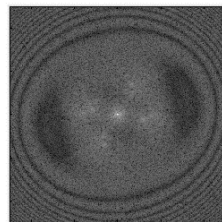
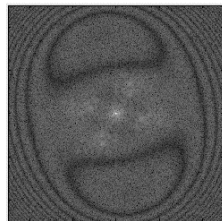


The Zemlin tableau is a series of diffractograms recorded at different illumination tilt angles. It allows evaluation of even and odd aberrations, which is not possible without tilt.



Tilt = $(-2, 0)$ mrad

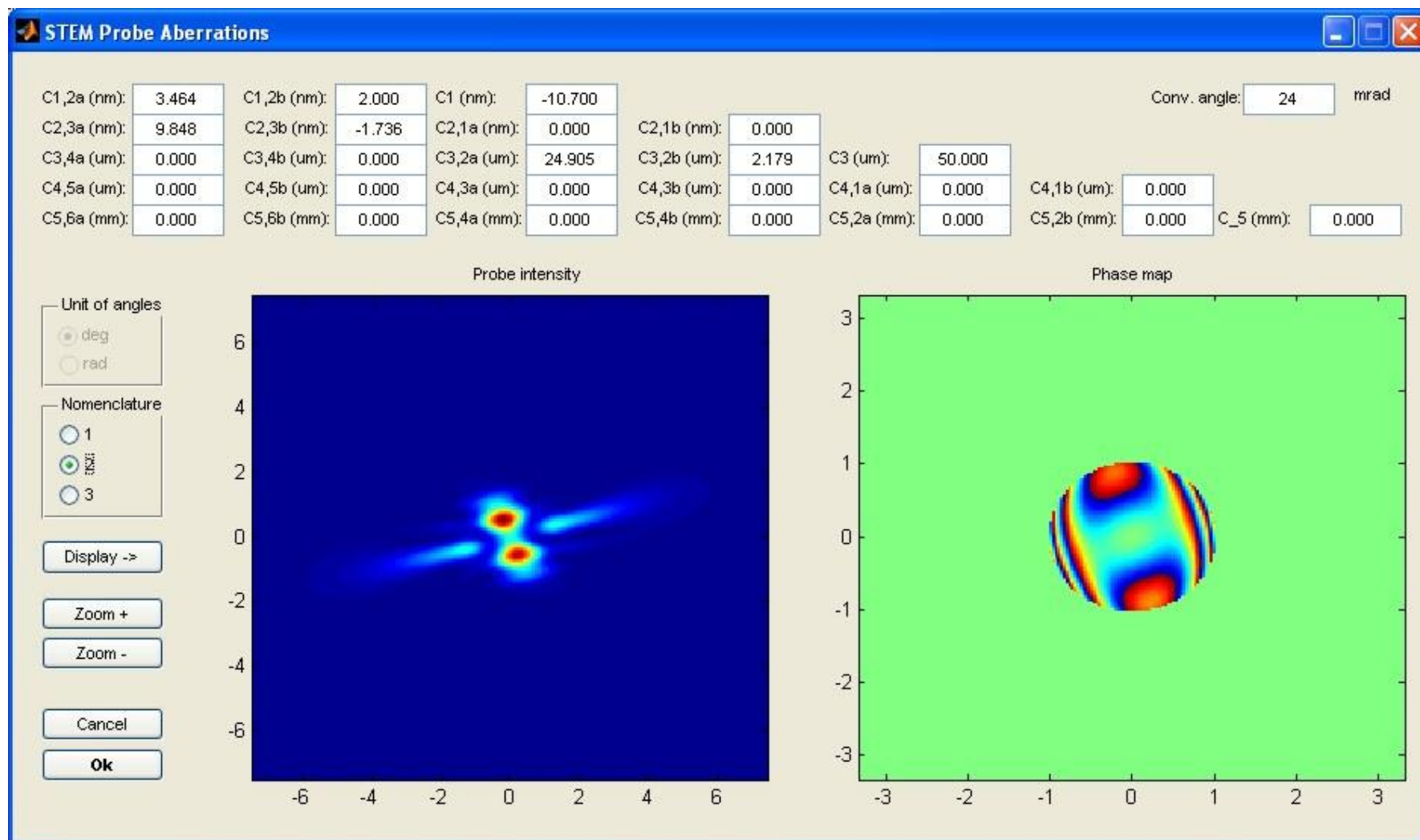
Tilt = $(2, 0)$ mrad



Tilt = $(0, -2)$ mrad

<input checked="" type="checkbox"/> Defocus	-65.7	nm		
<input checked="" type="checkbox"/> Cs:	1.2	mm		
<input checked="" type="checkbox"/> Astigmatism:	20	nm	<input type="text" value="0"/>	deg
<input type="checkbox"/> Field Curvature:	0			
<input checked="" type="checkbox"/> Coma:	10	um	<input type="text" value="25"/>	deg
<input checked="" type="checkbox"/> 3-fold Astigm.:	8	um	<input type="text" value="15"/>	deg

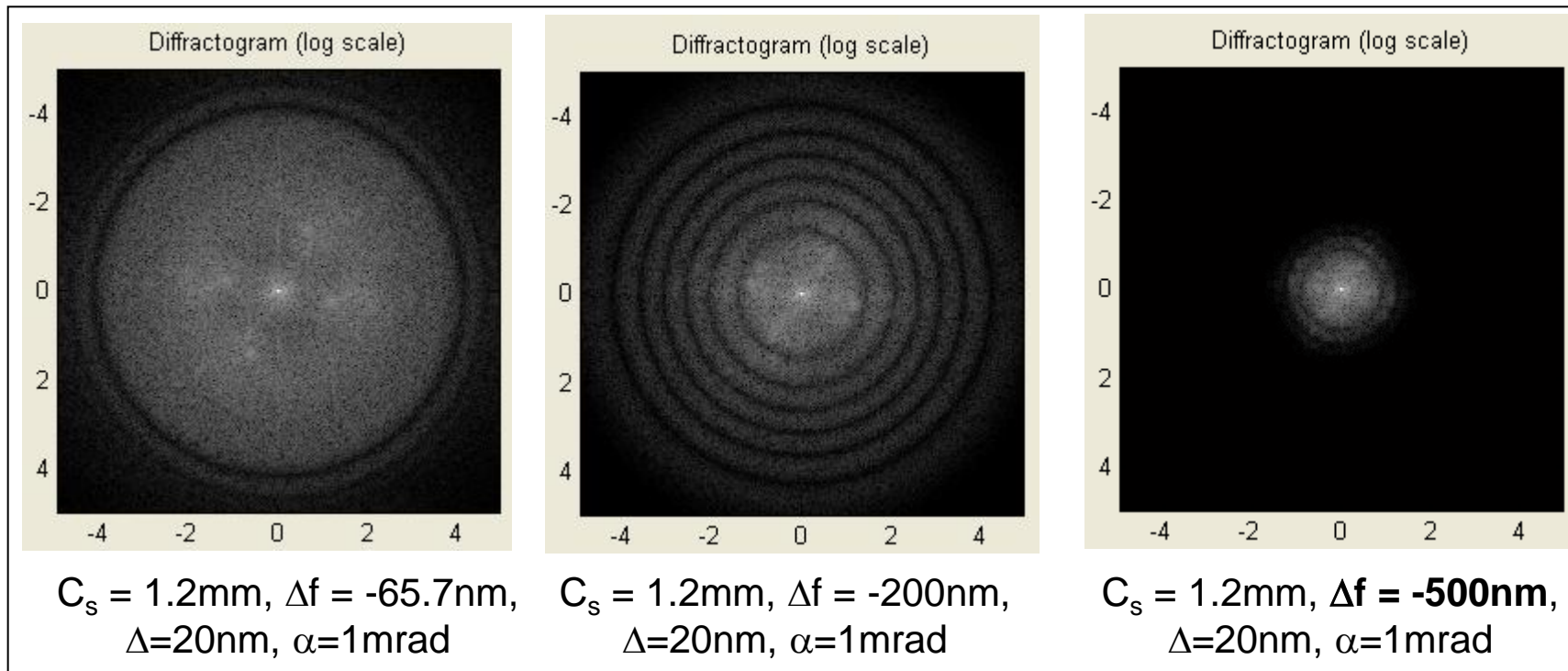
The Point Spread Function (PSF) of the STEM Probe



Shows what the Contrast Transfer Function (CTF) looks like in real space
(A STEM probe is the intensity of the PSF of the illumination system)

Effect of Partial Spatial Coherence in TEM

While coherent aberrations mangle amplitude and phase information in the images, partial coherence destroys information within the image all together.



Finite values of Δ and α are a result of limited (partial) **temporal (longitudinal)** and **spatial (transversal)** coherence as well as chromatic aberrations.

2) Partial spatial & temporal coherence in STEM and TEM

STEM

Partial temporal coherence

- Repeat calculation for range of different beam energies (can be done at no extra cost in frozen phonon calculation)

Partial spatial coherence

- Simple convolution of final image with the shape of the effective source

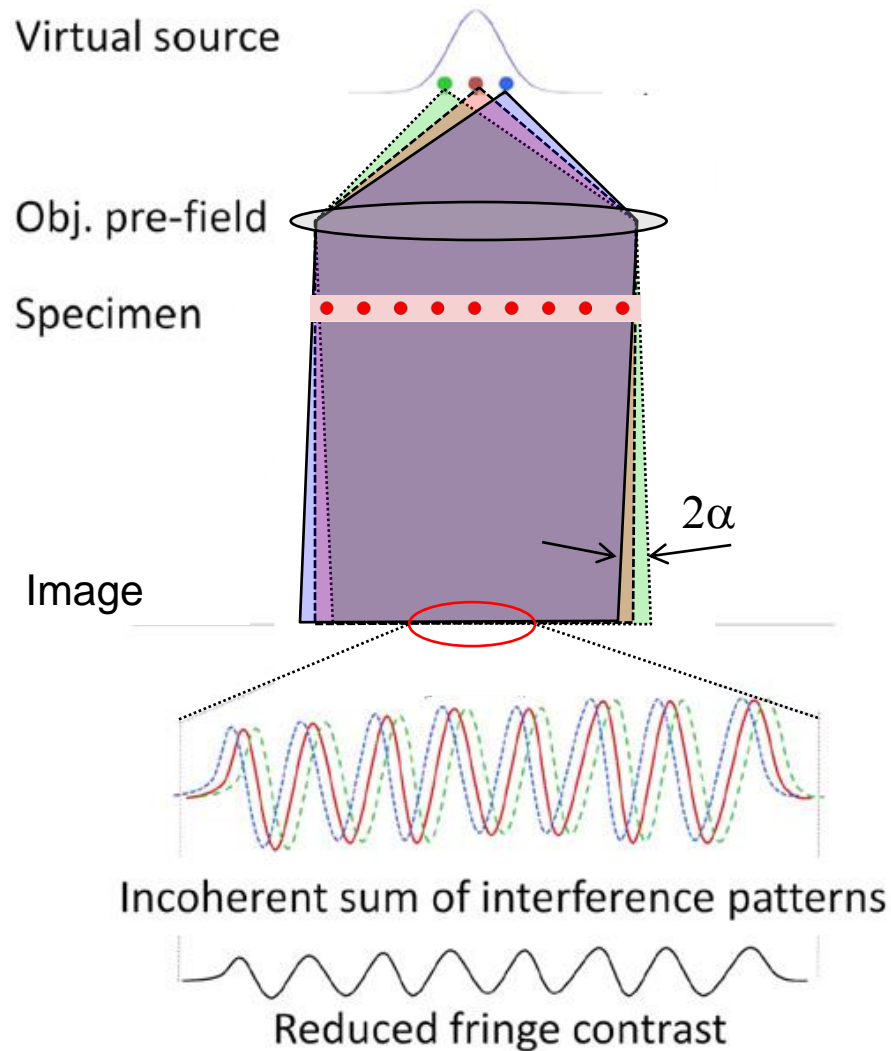
TEM

Partial temporal and spatial coherence should be included by numerical integration (repeating the simulation for different beam energies and angles of incidence)

- Quasi-coherent approximation (apply envelopes to wave function)
- Flux preserving approximation for partial spatial coherence => convolution of intensity by envelope function

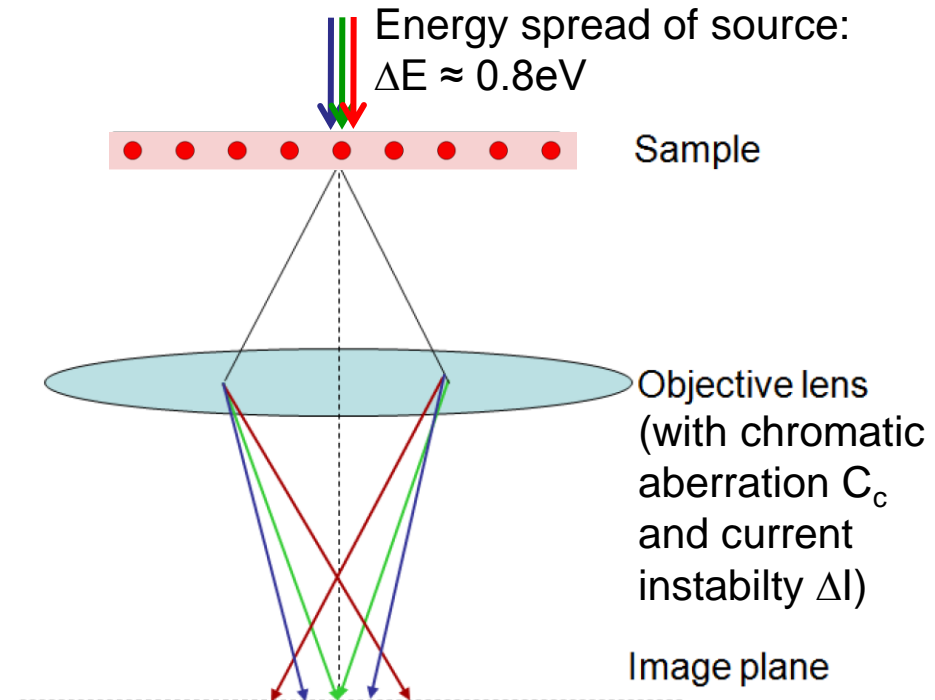
Partial Coherence in HRTEM

Partial spatial coherence



34

Partial temporal coherence



Parameters describing partial coherence

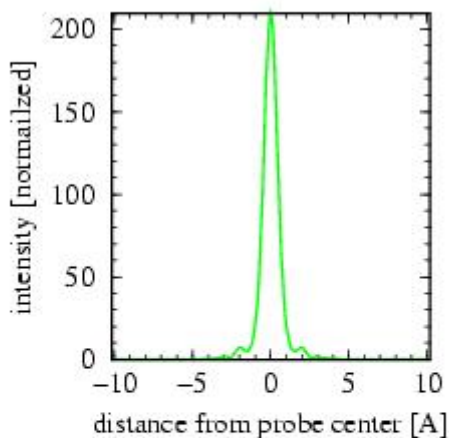
Spatial: illumination semi-convergence α

Temporal: focal spread $\Delta = C_c \sqrt{\frac{\Delta E^2}{E^2} + 2 \frac{\Delta I^2}{I^2}}$

Accounting for energy spread in STEM

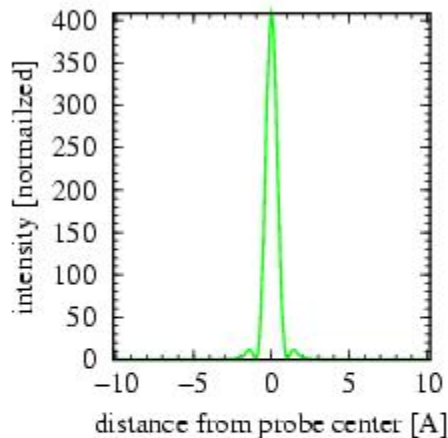
Incident probe intensity

dE: -0.43eV df: -65A



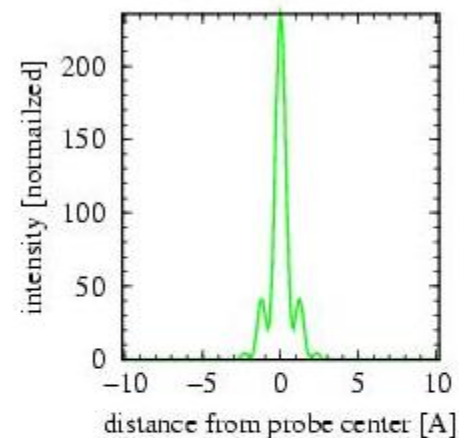
Incident probe intensity

dE: 0.00eV df: 0A

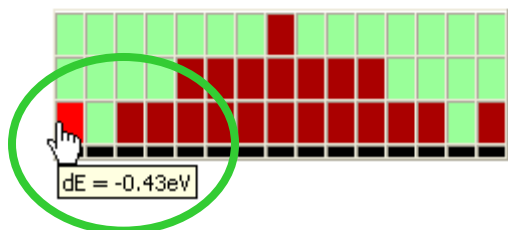


Incident probe intensity

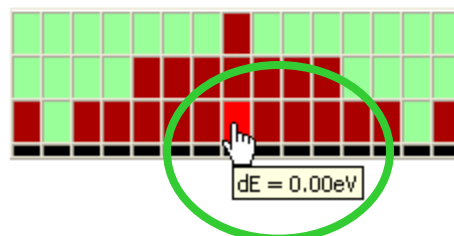
dE: 0.43eV df: 65A



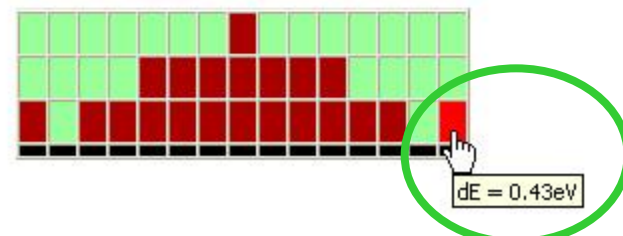
dE: -0.43 .. 0.43eV



dE: -0.43 .. 0.43eV



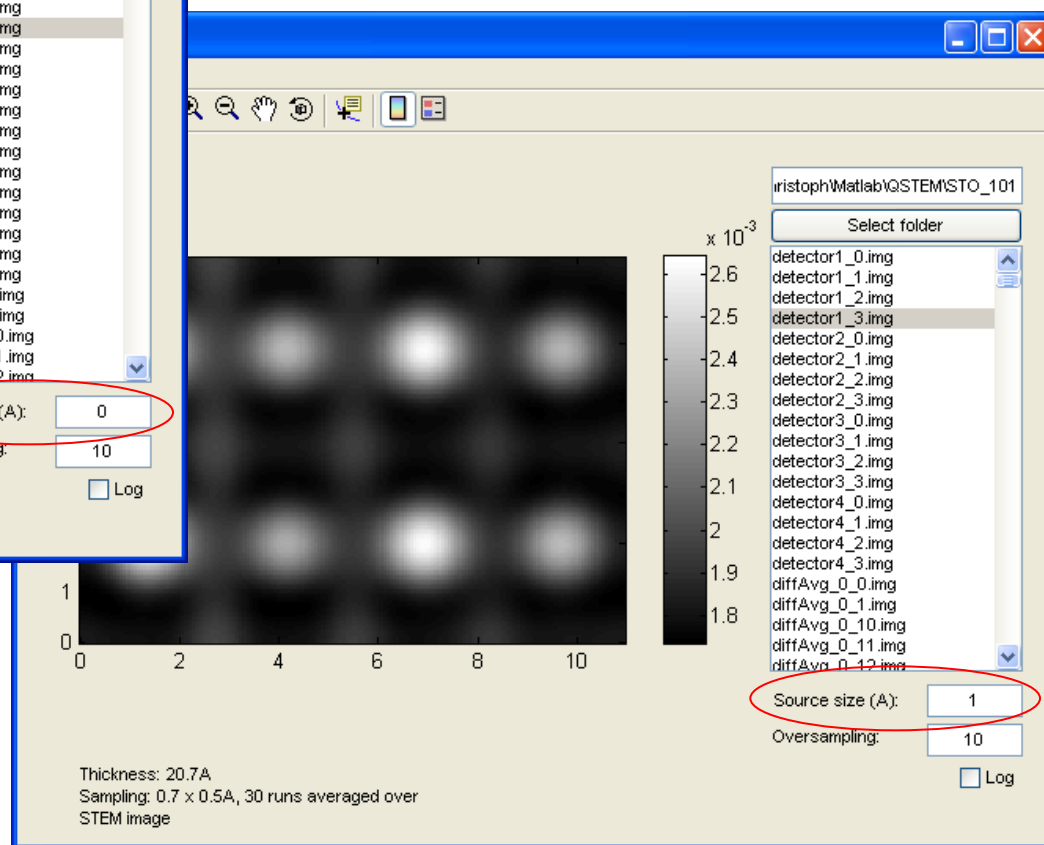
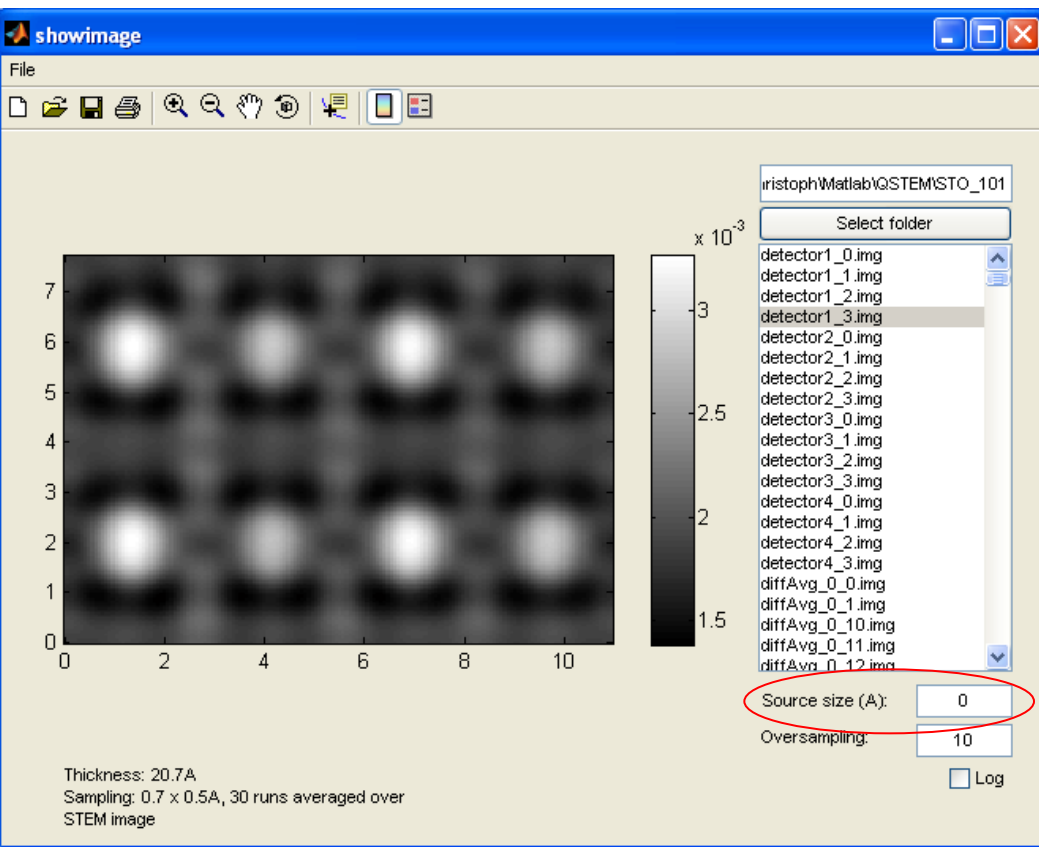
dE: -0.43 .. 0.43eV



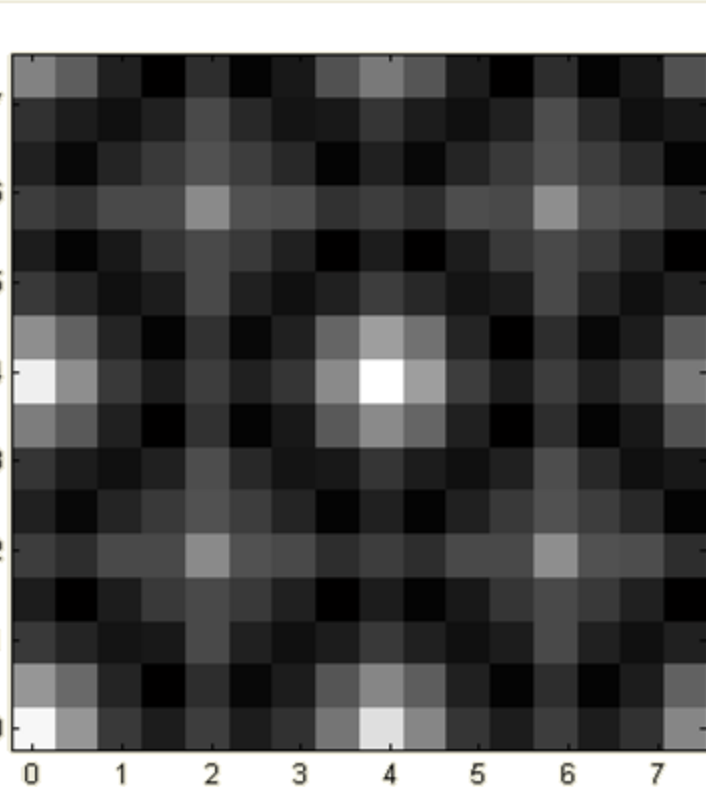
A Gaussian-shaped energy spread is taken into account by computing images at different energies (and with that defocus), as the different probe shapes above demonstrate.

Accounting for source size in STEM

The source size may be changed “on the fly” when displaying the images



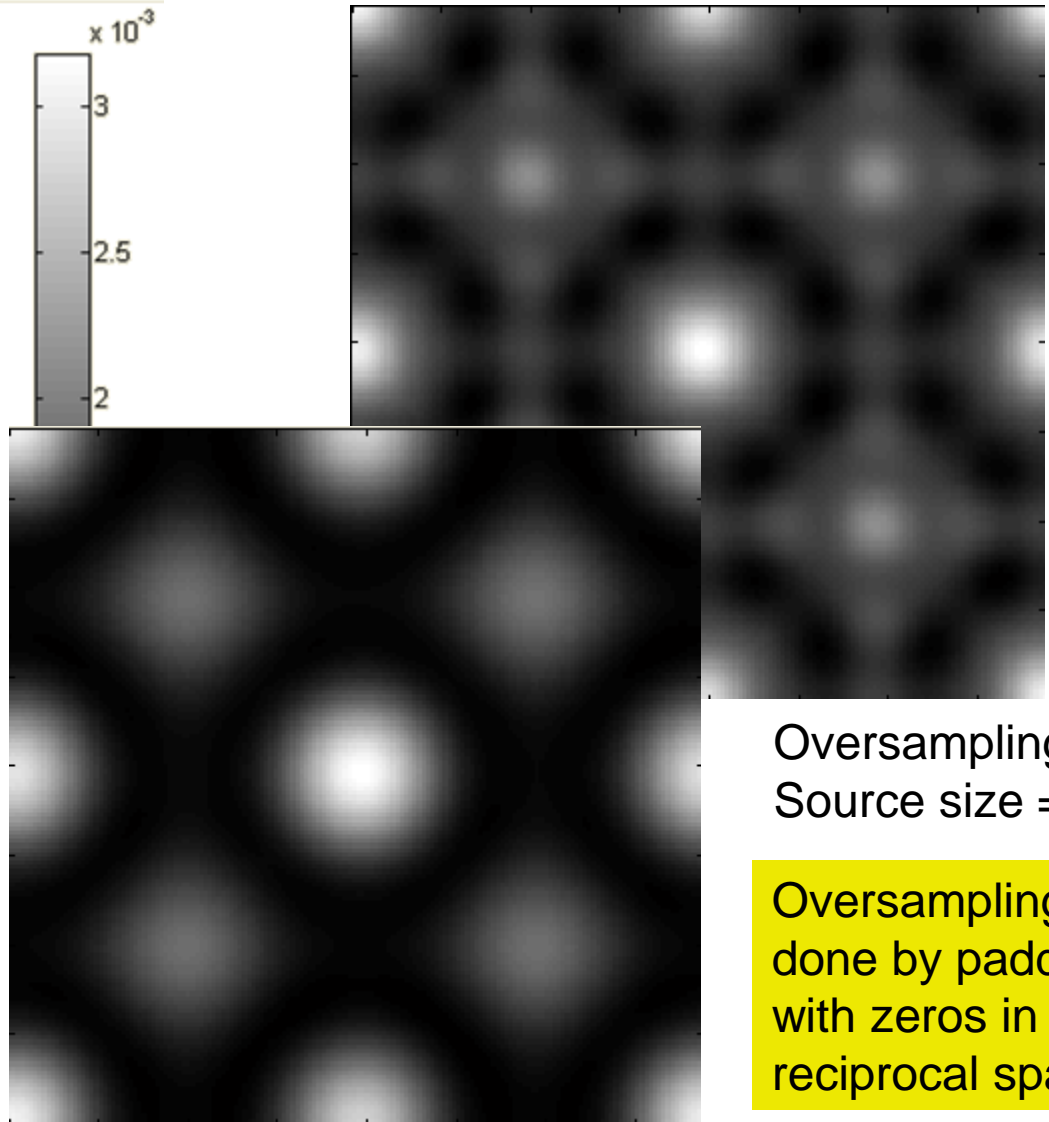
Interpolation between computed pixels in STEM



Image, as computed

Please be careful with
oversampling !!!

Oversampling = 10
Source size = 1A



Oversampling=10
Source size = 0

Oversampling is
done by padding
with zeros in
reciprocal space.

The Transfer Cross Coefficient (TCC) for TEM

$$I(\vec{r}) = \text{FT}^{-1} \left[\int \Psi_0(\vec{q} + \vec{q}') T(\vec{q} + \vec{q}', \vec{q}') \Psi_0^*(\vec{q}') d^2 \vec{q}' \right]$$

Transmission cross coefficient (TCC)

$$TCC(q + q', q') = T_{\Delta}(q + q', q') T_s(q + q', q') \\ \times \exp(-i[\chi(q + q') - \chi(q')])$$

Temp. Coherence: $T_{\Delta}(q + q', q') = \exp \left(-2(\pi \Delta f)^2 \left[\frac{\delta \chi(q + q')}{\delta \Delta f} - \frac{\delta \chi(q')}{\delta \Delta f} \right]^2 \right)$

Spatial Coherence: $T_s(q + q', q') = \exp \left(- \left(\frac{\alpha}{2\lambda} \right)^2 \left[\frac{\delta \chi(q + q')}{\delta(q + q')} - \frac{\delta \chi(q')}{\delta q'} \right]^2 \right)$

Coherent Transfer: $\chi(q) = \pi \lambda \Delta f q^2 + 0.5 \pi \lambda^3 C_s q^4 + \dots$

The quasi-coherent approximation

Spatial Coherence Envelope Function: $E_s(q) = \exp\left(-\left(\frac{\alpha}{2\lambda} \frac{\delta\chi(q)}{\delta q}\right)^2\right)$

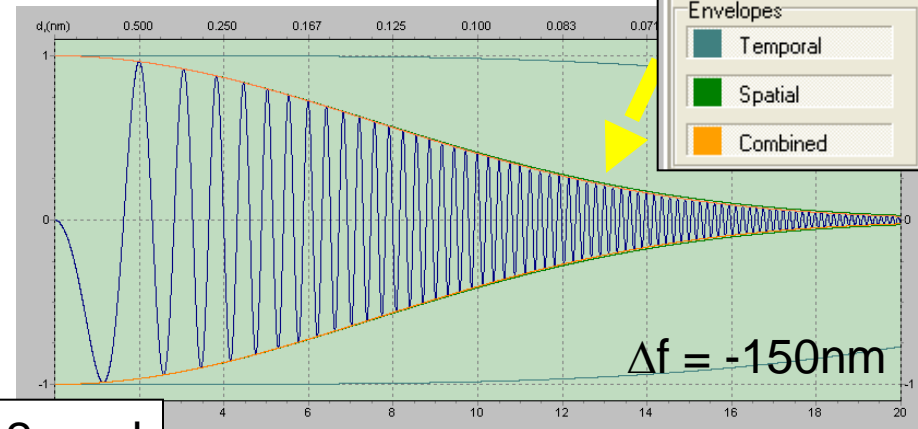
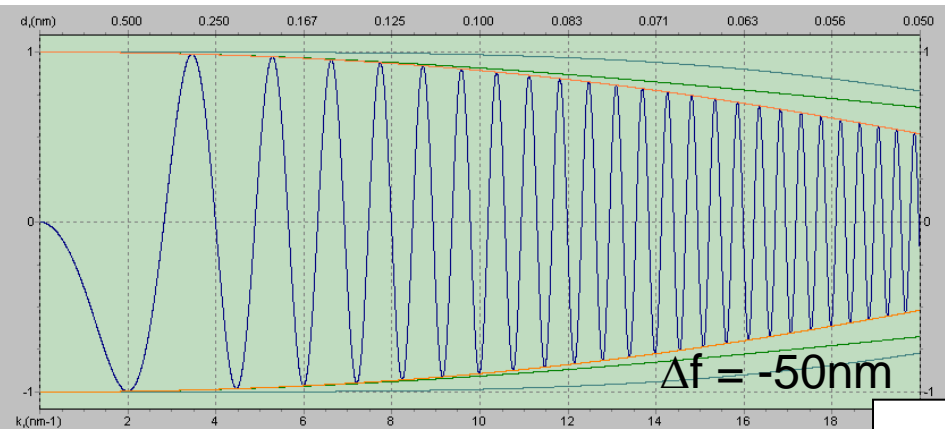
Temporal Coherence Envelope Function: $E_\Delta(q) = \exp\left(-2(\pi\Delta f)^2 \left[\frac{\delta\chi(q')}{\delta\Delta f}\right]^2\right)$

$$I(\vec{r}) = \left| \text{FT}^{-1} [\Psi_0(\vec{q}) \exp(-i\chi(q)) E_\Delta(q) E_s(q)] \right|^2$$

Problem: Multiplying the complex wave function with an envelope cuts away electrons!
(which is unphysical)

Will assume:

1. (dispersion free) monochromator: energy width 90meV => neglect $T_\Delta(q+q',q')$
2. C_s -corrector => $\chi(q) = \pi \cdot \lambda \cdot \Delta f \cdot q^2$

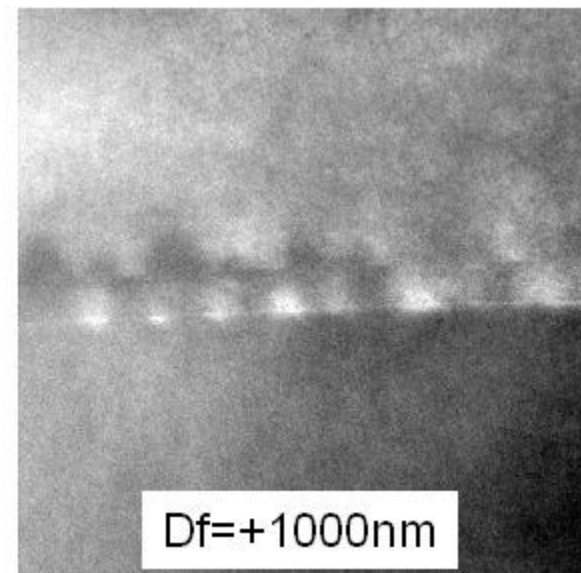
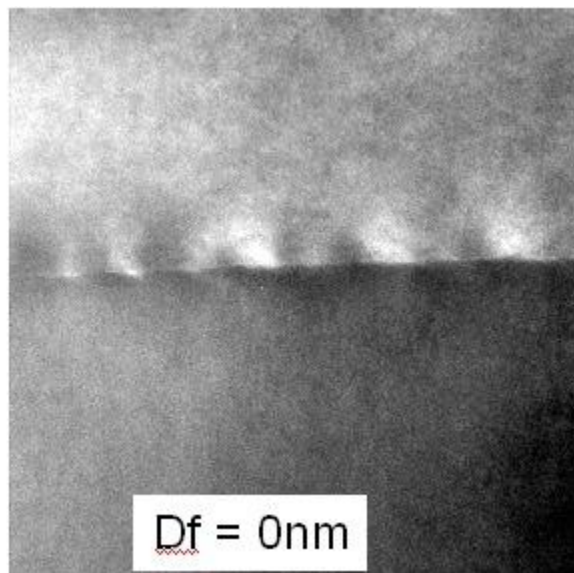
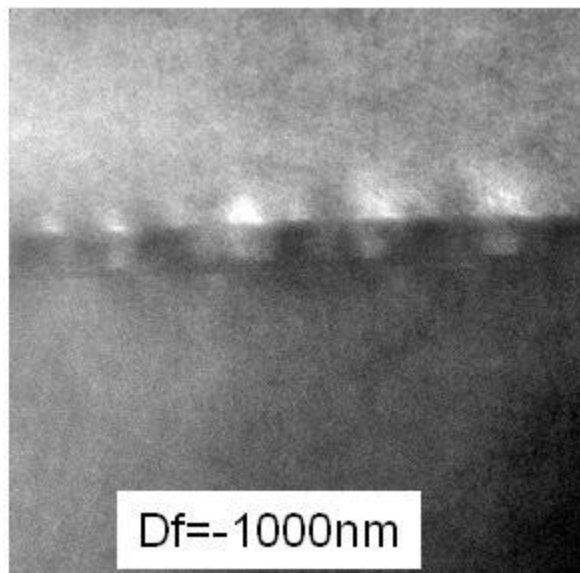


$\alpha = 0.2\text{mrad}$

Flux preservation important at large Δf

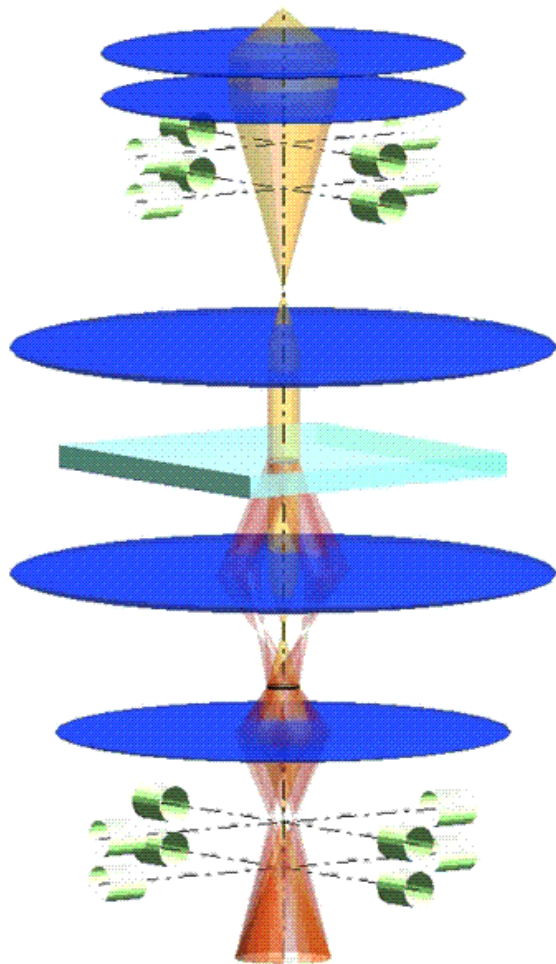
The **TCC** correctly predicts the presence of
DF images in defocused BF images

(in the quasi-coherent approximation these electrons would be missing)



Experimental BF images of a $\Sigma 5$ grain boundary in SrTiO₃.
Large Objective aperture, relatively large convergence angle.

Thank You!



SpotMode = 0.0, DiffMode = 0.0

